Multi-body Dynamic Analysis of a Railway Passenger Car

Jorge Afonso Hora de Carvalho Martins

Master Dissertation

Supervisor: Prof. Abílio de Jesus

Co-Supervisor: Prof. Cláudio Horas

Co-Supervisor: Prof. Francisco Pires

U.PORTO

FEUP FACULDADE DE ENGENHARIA UNIVERSIDADE DO PORTO

Masters in Mechanical Engineering

September 2023

Middle of adventure, such a great place to start

-Arctic Monkeys

Resumo

Esta dissertação pretende desenvolver um modelo de dinâmica multi-corpo que represente o comportamento dinâmico das carruagens ARCO da CP. A Comissão Europeia, no *The European Green Deal*, prevê um aumento significativo do transporte ferroviário, o que implicará um aumento da procura de material circulante. Nesse sentido, Portugal está a procurar desenvolver novo material circulante fabricado nacionalmente. O aumento dos últimos anos da procura pelo transporte ferroviário levou a CP a adquirir as referidas carruagens à operadora ferroviária RENFE no estado usado. Ademais, este trabalho pretende ser exploratório para o papel que a Faculdade de Engenharia terá no projeto PRR para o desenvolvimento de material circulante em Portugal. Sendo a análise dinâmica uma parte fundamental do desenvolvimento de material circulante ferroviário, é também para a FEUP importante desenvolver conhecimento nessa área e na qual surge esta dissertação.

Nesse contexto, esta dissertação começa por fazer um resumo da evolução dos caminhos de ferro, começando por vagões de transporte de carvão sobre travessas de madeira, tracionada pela gravidade e por cavalos, até à atualidade e ao desenvolvimento da alta velocidade. É também abordada a história da dinâmica de veículos ferroviários como área científica e da história ferroviária em Portugal. Finalmente, é feita uma análise dos passos e estratégias necessárias ao projeto de um veículo ferroviário, assim como as normas aplicáveis.

São também explicados os principais princípios teóricos por detrás da dinâmica multi-corpo. É dado um especial foco às estratégias e ferramentas desenvolvidas para modelar os diferentes componentes do veículo.

O principal foco da dissertação consiste no desenvolvimento de um modelo de uma carruagem no software comercial SimPack, sendo para isso analisados os princípios base deste tipo de modelo e as alternativas de modelação dos diversos elementos. Assim, foi desenvolvido um modelo das carruagens ARCO, baseando o presente trabalho num caso de estudo real, algo que influência também as análises e resultados pretendidos. Assim, serão feitas as simulações previstas na norma EN 14363, uma análise de conforto de passageiros numa linha reta com irregularidades, a determinação da velocidade crítica do veículo com e sem amortecedores anti-lacete e ainda a análise do comportamento do veículo num troço da Linha do Norte onde ocorreu um incidente.

A partir das diferentes análises, conclui-se que o modelo permite obter resultados garante uma performance superior aos impostos à circulação, no caso da velocidade critica, de 390 km/h. No entanto, em termos de comportamento dinâmico este fica aquém daquelas que são as características das carruagens ARCO, considerando que à velocidade de 200 km/h ocorre um descarrilamento em curvas com raio inferior a 400 m. Para além disso a forças laterais transmitidas aos carris são superiores às definidas na norma

Abstract

This dissertation aims at developing a multi-body dynamic models to represent the dynamic behaviour of ARCO passenger car, from C.P. The European Commission, in the background of “The European Green Deal”, predicts a significant increase in rail passengers transportion, which will mean an increase in demand of rolling stock. For that reason, Portugal is aiming at developing new rolling stock manufactured or retrofitted nationally. The increase in demand for rail transport has led C.P. to acquire the ARCO rail car. This are used rail cars from RENFE, the Spanish rail operator. This work is also framed in the role that FEUP will play in the *PRR* project for the development of rolling stock in Portugal. Being dynamic analysis a fundamental component in the development of rolling stock is fundamental for FEUP to create knowledge in this area justifying this dissertation work.

The entrance in Portugal of a different model of rolling stock, appears as an opportunity for a case study in the development of multi-body dynamic models. So, this thesis starts by making a summary of railway history, from wagons on wooden rails to transport coal using gravity and horses until the current days and the development of high-speed railways. It is also displayed the development of rail vehicle dynamic as a scientific area of expertise and the Portuguese railway history. Finally, an overview of the steps and correct strategies to develop a rail vehicle project is done, as well as the necessary standards and regulations.

The basic theoretical principles behind multi-body dynamics are also explained. It is given special focus to the strategies and tools already developed in the literature for modelling the different components of the vehicle.

The main focus of this work is the development of a rail car model using the commercial software SimPack. With that in mind the main principles behind this type of models and the many alternatives for the modulation of the several elements are analysed. Thus, a model of the ARCO was developed, as well as defined the type of simulations to be carried out. Thus, the simulations according to in the EN 14363 standard will be carried out, an analysis of passenger comfort on a straight line with irregularities, the determination of the vehicle's critical speed with and without anti-yaw dampers and the analysis of the vehicle's behaviour on a section of the *Linha do Norte* where an incident occurred.

From the different analyses, it can be concluded that the model predicts, including better results than the real situation, such as critical speed. However, in terms of dynamic behaviour it falls short of those that are the characteristics of ARCO carriages.

Acknowledgements

Finishing a degree and in particular a master thesis is not something possible to do alone. For that reason, I would like to thank, firstly my supervisors Professor Abilio de Jesus and Professor Claudio Horas and Professor Francisco Pires, for the support and availability to together understand the problems in the model and combining knowledge to solve them. I would like to, in particular, thank Professor Abílio de Jesus for the proposition of developing this theme and specialty for welcoming me to the world of the railway.

The most special acknowledgement goes to my parents, whose support and role model was indispensable to me to conclude my degree in Engineering. I would also like to thank my entire family: aunts, uncles, grandparents, and sister.

Finally, my last acknowledgement goes to those with whom I shared the last 5 years. College is a time for challenging ourselves and together with all those who surround us overcome challenges we did not know existed. Either in the academic traditions or in NEEM, is the teamwork that makes the whole experience possible. I must name specialty Manuel Henrique, Jorge Paiva e Ana Pinheiro, my partners for the last two years, together we accepted the challenge of attending the first class of the master's specialization in Aeronautical structures. Many papers after, many nights after, many difficulties after, what will stand will be the capacity that we had of making the whole more than the sum of the parts.

This work is a result of Agenda "PRODUCING RAILWAY ROLLING STOCK IN PORTUGAL", nr. C645644454-00000065, investment project nr. 55, financed by the Recovery and Resilience Plan (PRR) and by European Union - NextGeneration EU

PRR Plano de Recuperação e Resiliência

REPÚBLICA PORTUGUESA

Financiado pela União Europeia NextGenerationEU

This work is a result of project "FERROVIA 4.0", with reference POCI-01-0247-FEDER-046111, co-funded by the European Regional Development Fund (ERDF), through the Operational Programme for Competitiveness and Internationalization (COMPETE 2020) and the Lisbon Regional Operational Programme (LISBOA 2020), under the PORTUGAL 2020 Partnership Agreement.

Lisb@20[20] COMPETE 2020 PORTUGAL 2020 UNIÃO EUROPEIA Fundo Europeu de Desenvolvimento Regional

FERROVIA 4.0

Contents

List of figures

List of Tables

1 Introduction

Multi-body dynamics are a relevant part of the development of railway rolling stock. The increase in demand for rolling stock means an opportunity to develop of knowledge and boost the level of expertise in Portugal and at FEUP.

1.1 Context

In recent years, there have been several investment commitments in the railway sector, both at national and European level. In the European Green Deal, the European Commission (EU) establishes as a goal to double the traffic in High-Speed by 2030 and to double the freight traffic by 2050. Portugal is evaluating the anticipation of this goal to 2045, in which a modal change to railway will play a fundamental role [1-3].

One of the most fundamental pieces of EU policy in terms of transportation and mobility is the Trans European Network (TEN-T). In terms of rail transportations, it is composed by two layers [4]:

- Core Network, which includes the most important connections between the larger cities. It must comply with the highest standards and be completed by 2030;
- Comprehensive network, which includes connections between all regions and the core network, it needs to be completed by 2050.

In 2022, a revision to this policy was proposed containing an intermediate layer, which should be completed by 2040, with an increase ambition regarding sustainability and the climate crisis. In Figure 1, the railway TEN-T, is outlined. Besides the planning of the network, this policy also includes infrastructure standards to be complied, in order to ensure the interoperability of every national network [4]. Figure 1 also shows that this network will include various types of infrastructure in terms of maximum speed and type of traffic.

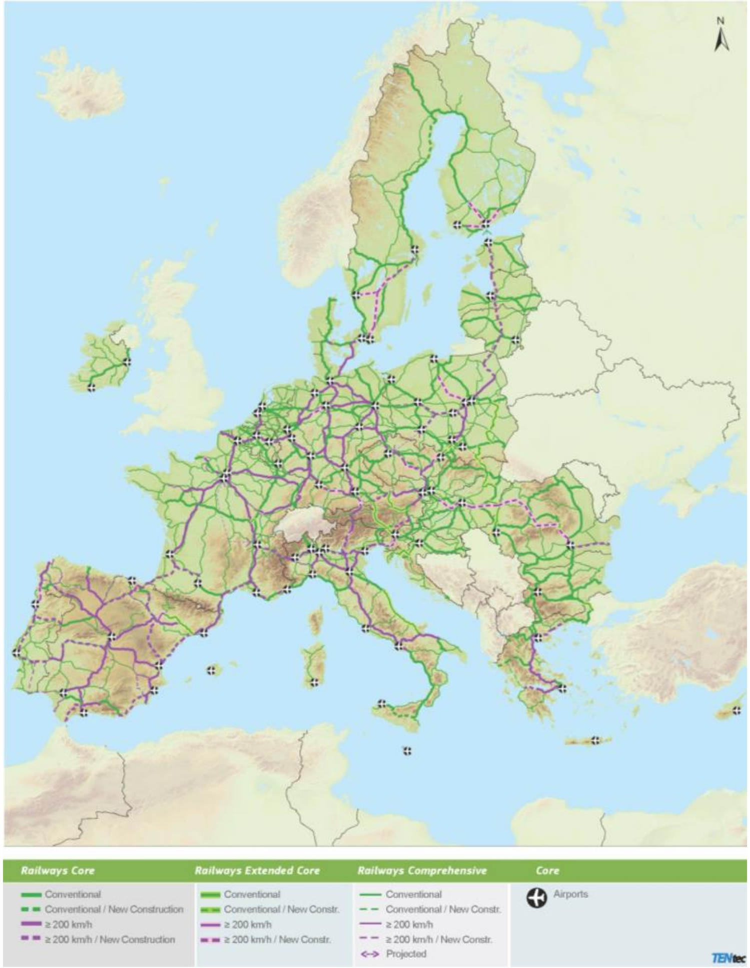

Figure 1 - TEN-T with both comprehensive and core layers, regarding railway [4].

The Portuguese government has also designed several strategies for the sector. For the first time, in recent years, Portugal is creating a National Railway Plan (*Plano Ferroviário Nacional*). Several investments have also been announced both in infrastructure and rolling stock and some of them are already ongoing. These are put in place by the two national companies, *CP - Comboios de Portugal, E.P.E.* and *IP - Infraestruturas de Portugal S.A.* (IP) [5].

Currently there are 2 fundamental investment programs underway. The *Ferrovia 2020,* which was planned to be completed in 2020, but several projects are still in progress, with a total investment planned of 1.019 B€ and its main objective is to improve the freight capacity of the infrastructure [6, 7]. The other fundamental program is *Programa Nacional de Investimento 2030,* with a total investment of 10 B€, focused on improving the passenger transportation capacity and maximum infrastructure speeds [8].

Finally, several institutions, both companies and public entities have joint to develop a new Portuguese passenger rail car. This is a projected funded by the European Union by the Next Generation EU funding. The project is called *Produzir material circulante ferroviário em Portugal* (in English, Manufacturing railway rolling stock in Portugal). This aims manufacturing 3 rail cars, with a budget of 36.7 M€. FEUP is a part of the project and the knowledge and experience gained with this dissertation will be relevant for the participation in the project [9].

CP - Comboios de Portugal, E.P.E. (CP) is the national rail operator in Portugal, transporting 148.1 million Passengers/year. Legally, it is a statutory company, having as only share holder the Portuguese state, under the responsibility of both the Ministry of Infrastructure and Ministry of Finance.

In 2019, CP signed a Public Service Agreement (PSA) with the state, which covers all services operating at a loss in Portugal. Currently, the 2022-2030 strategic plan includes the modernization of the company, focusing on innovation; improving the customer experience and the rail offer; prepare a new PSA and prepare for High-speed rail. CP has, for the first time, ended 2022 with profits [10, 11].

Regarding rolling stock, there are several planned investments in a great quantity of new rolling stock for the national company, CP. Those are:

- 22 Electrical Multiple Units (EMUs) for regional transportation (public tender won by Stadler) [12];
- 117 EMUs for regional and suburban services [13];
- 12 high speed EMUs (public tender delayed, matching infrastructure schedule) [14].

However, there is a current need to renew the company rolling stock, these orders will take at least until 2026 to arrive. To solve this problem a different solution was needed, which originated a new policy. With the integration of the maintenance company EMEF CP had an increase engineering capacity. This allowed it to renew old, decommissioned rolling stock, in 2019, was presented a plan to renovate 168 units (both carriages, locomotives and multiple units) [15, 16].

1.2 Objectives

The main objective of this dissertation is the development of a rigid multi-body dynamics model of the ARCO passenger car, from CP rolling stock. Furthermore, achieving this goal will require an increase in the level of knowledge about multibody dynamics at FEUP. The increase in the development and investment in the rail industry will require a development of the capacity and level of knowledge in the institution. This thesis also aims to aggregate the basic facts and figures of the rail industry and rail rolling stock design.

From the developed is a key goal the analysis of the dynamic behaviour of the model and predict its correlation with the real ARCO passenger cars.

Finally, an important goal of this dissertation is to explain the main requirements and necessary data and the necessary steps that should be taken to build a similar model. Furthermore, the model built seeks to be as parametric as possible, allowing for, with simple alterations, model a different rail car.

1.3 Contribution to science

Recently, Multi-body dynamics analysis has been subject to several studies, which will be explored in Chapter 2. The development of more concrete cases and different rail car will contribute to the improvement of the reliability of this analysis. Furthermore, as the Portuguese industry aims at developing new Portuguese rolling stock, the analysis of current models is essential to develop new ones.

1.4 Dissertation structure

This chapter introduces the work carried out, highlighting the contributions to science, and disclosing the contents of this document.

Chapter 2 will consist of a review on the railway history, some important facts about the reality and perspective of the railway industry, especially in Europe. In the same chapter will also be done an overview of the rail car design and the most relevant standards and regulations, they must obey.

Furthermore, in Chapter 3 will be done a state-of-the-art review regarding multibody dynamics, the theoretical description, as well as several examples of works done in this subject. These examples will be relevant to develop the analysis done to the developed model.

Chapter 4 consists of the description of the ARCO railway car and the necessary considerations and data used to build the model. The final characteristics defined, and the steps taken in the multi-body dynamics commercial software will be described.

Additionally, Chapter 5 consist, firstly, in the analyses and tests to which the model was subjected to, followed by the analysis of the results. This chapter will describe the results obtained in the simulation, as well as comparing them with examples from the literature, which will allow for an understanding of the plausibility and accuracy of the results in a real situation, since there is some lack of data on the train model.

Finally, in Chapter 6, several conclusions will be drawn about the model and its development stages, and future work will be discussed.

2 The Railroad

This chapter summarises the history of the railways and the railway industry. In addition, the most relevant characteristics of modern passenger rolling stock will be analysed, as well as a brief overview of the next possible developments in rail technology.

2.1 From the beginning until the XX century

2.1.1 From the beginnings to the iron rails

Although not a form of railway exactly as those seen nowadays, around 600 BC in Ancient Greece a predecessor of the railway system can be seen. The Corinthians built a series of grooves dog in the ground. The so-called Diolkos was built on a paved route of around 6 kilometres and was used to guide the carts that transported bouts. This was a much faster rout to cross the Isthmus of Corinth than sailing around the Peloponnese peninsula [17, 18].

During the next centuries waterways were the most used mean of transportation to move heavy items in bulk. However, the characteristics of the metals required a new solution for transporting large quantities of material. in the 16th century, due to the increase in metal extraction and in places where transport by river was not practical, a new solution was needed to transport a large quantity of ore.

This solution consisted of building rails for the wheels to move with little friction and to reduce the volume of construction, two parallel rails, usually made of wood, were used. This were guided with flanges either in the rails or in the wheels. To move the wagon gravity was used when fool and horses used to lift back the empty wagon. In Figure 2 a replica of these wagons can be seen [18-20].

Figure 2 – Replica of wooden mineral wagon and track displayed on the Tanfield Railway in County Durham [19].

Wear and tear due to wood-to-wood contact led to the frequent need to replace sleepers and rails. The increase in iron production resulted in the upgrade of the wooden rails and wheels to iron ones. Cast iron rails first appeared in 1729 and by 1760 they were widely present. The older version was still based on rails completely supported by wooden boards. In order to continually reduce costs, the first autonomous cast iron rails were developed. Although, having better strength, durability and traction resistance properties, this material was still prone to fracture under excessive loads [17, 19].

The turn to the XIX century brings a new paradigm change to the railway industry. With the increase of iron and coal production and the industries desire to reduce transportation costs led to rails shapes diversification and development, reducing friction further. This allowed longer trains, reducing the operating costs. At this time traction was still done by horses on empty trains and gravity allowed the move of full trains, which limited the topography of the rail lines [19].

2.1.2 Steam locomotive

The need to overcome steeper gradients was the reason for replacing horses with rope winding cylinders, power by steam engines. These appeared around 1805, and maintained the descending loaded wagons, changing how they were ascended [19].

Around the same time, Richard Trevithick developed a high-pressure, steam engine (2-3 bar), shown in Figure 3. This was smaller and easier to install than the previous engines. On the 21st of February 1804, he mounted the engine on a car, developing a 7-ton locomotive, which travelled a 13 km journey between ironworks and the Merthyr-Cardiff Canal at Abercynon. The train was composed of a locomotive hauling 70 passengers and 10 ton of iron, in five wagons and reached almost the speed of 8 km/h [17, 20, 21].

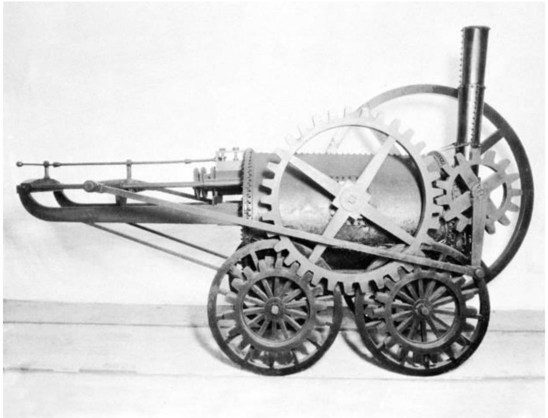

Figure 3 - Steam power locomotive developed by Richard Trevithick [20].

In the following years, other engineers developed new locomotives, such as, John Blenkinson, Matthew Murray, William Hedley Christopher Blacket and George Stephenson. In 1825, a train was operating at 35 km/h, transporting passengers between Sotckton and Darlington [22].

2.1.3 Development of rail networks

The development of the steam locomotive simultaneously with the appearance of iron wagonway resulted in a revolutionary change in transportation infrastructure. The combination of both developments led to an increase of 1.3 million km, in 57 years around the world. The railway expansion happened mostly geographically, i.e., countries closer to England showed a quicker increase in rail infrastructure [23].

The next phase in railway development occurred around Europe with similar intensity, although, in different manners. While in England the rail infrastructure construction was led by private companies, in the rest of Europe the construction and planning of the infrastructure was done by public owned companies or private companies financed by the state [23, 24].

This is also known as the Golden Age of Rail, beside the quick construction of intercity rail lines, it was in the end of the XIX century that several urban transportations were implemented. However, the maximum railway infrastructure would be reached around the 1930s, and the total length of the lines would decrease in several countries in the following years due to the introduction of cars [23, 24].

2.1.4 Introduction of electrical traction

Between 1790 and 1840, several scientists preformed experiments on the use of electrical power to produce motion, which resulted in small low power and unreliable motors. In the 1840s, electrical locomotives were shown possible, however, the use of batteries as power source was a limitation. The excessive weight of the locomotives would lead to a small range [20, 25, 26].

In 1851, a fundamental development took place: the use of railway tracks to transmit energy was proposed and various experiments were carried out. On one hand, it was shown the possibility of providing power without moving the source; on the other, until this technology was possible, took 30 years. The low quality of the several electrical components was the main reason [20, 26].

In 1879, the first electric locomotive was presented at the Berlin Industrial Exhibition. During the next years, several European countries would invest in their infrastructure, making available the use of electric traction. Electrical power was then mainly used on main lines our in high demand commuter lines [19].

Since the use of batteries was abandoned, the power needed to be transmitted to the locomotive. For these several options were developed, both in the means of transmission and the electrical current used. Overhead cables or active third rail were the most common options for transmission of the electrical power to the locomotive. Regarding the electrical current, it was initially used mono phase alternating current at 16 2/3 Hz. The most widespread electrification was low voltage direct current, specially, since the first electrically powered rail systems were for urban transport. After the world war alternating current at industrial frequencies was adopted [25].

2.1.5 Introduction of Diesel traction

The first diesel locomotive was developed by Rudolf Diesel, Adolf Klose, and Gebrüder Sulzer, in Switzerland in 1906. However, in 1888, William Thomson tested the use of a 2-cylinder petroleum engine on rails, showing the technology capacity. The first diesel locomotive was tested in a main line, in 1912. The first examples showed high cost per power ratio, high maintenance cost and had complication regarding power transmissions. The development of Diesel-electric locomotive allowed an easier control of the diesel power and the energy transmission problem, which was done by Hermann Lemp, in 1914 [20, 27, 28].

Nevertheless, diesel locomotives had a bigger initial cost compared to steam locomotives, despite having higher capacity and lower operating costs. These became more competitive in the 1930s and a quick change happened in the United States. In Europe, due to the financial capacity required and the impact of the 2 world wars led to a delay in this upgrade, occurring in the 1960s. An exception was the use of diesel locomotive for shunting, small and low speed trips, where even mechanical transmission is used [20, 27, 28].

Diesel was less efficient compared to electric traction but did not require the large initial investment in infrastructure. However, in main lines with great use, electrical traction would be the best option. This means diesel would only replace steam locomotives, powered by coal. Gas turbine engines were also studied but did not show any success [20, 27, 28].

2.2 History of research into railway dynamics

The analysis of a wheelset running on tracks is a complex mathematical problem. The first analysis done about this problem happened in the XIX century. Due to the poor material quality, this analysis was important to determine the construction of both the wheels and the track, considering dynamic loads, which was done empirically. The second problem was the ability of wheels traveling along the rail path, solved by flanging the wheels. Later more precise analysis were done [29-31].

The first formulation of the wheel-rail kinematics was done by George Stephenson, the principle of the double cone. This principle consisted of considering the wheels as cone sections with smaller inner diameter, than outer. In the case of an irregularity, this will cause different diameters on each side, creating an imbalance, which will force the opposite movement, resulting in a similar destabilisation of the system, creating an oscillatory movement [32].

This formulation was the base for the research of Ferdinand Redtenbacher, who tried to explain the wheelset behaviour during the inscription in curves. Redtenbacher enhanced the understanding of the contact problem, stating the deformation of the wheel and rail in the contact [30, 33, 34].

In 1883, Johan Klingen developed the mathematical formulation of Stephenson's problem, trying to determine the wavelength of this oscillation, which is called Hunting motion. With regard to the stability of this movement, a few years later Christoph Boedecker produced a similar model, but with one crucial difference: he introduced physical relationships into the contact using Coulomb's law. In addition, this researcher came to a conclusion about the stability of the train. concluding that the wheelset is always unstable, derailment is only prevented by the wheel flanges [31, 34-36].

In 1926, Carter succeeded for the first time in analytically establishing a relationship between the rail and the wheel. His formulation was able to determine the local creepage, contact stresses and creep forces. The analysis determined a proportional relation between creep and the tangential and longitudinal forces [34].

2.2.1 Post WWII developments

After the Second World War, both Japan and France began developing high-speed trains. Progress made in Japan took some time to reach Europe, as Japanese papers were written in Japanese. In France, in the first test, the train reached the speed of 331 km/h. However, the track suffered several damages as shown in Figure 4 [30].

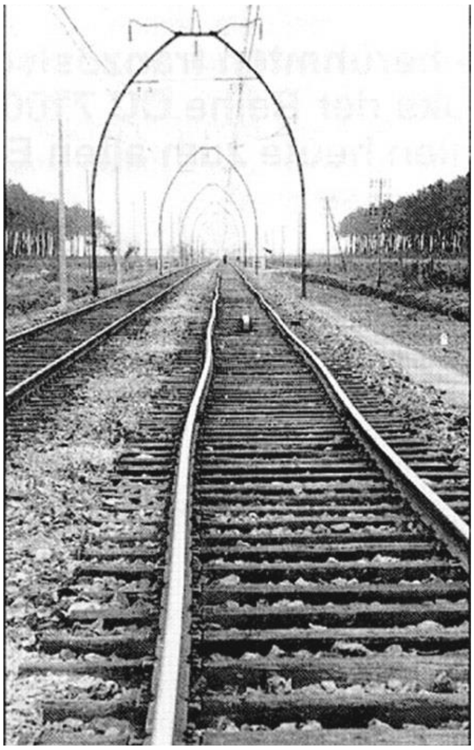

Figure 4 - Railway track after the first high speed test by SNCF[30].

The most logical explanation for this event is that the train was running unstably, increasing the lateral loads on the rails. Another explanation is the fact that maintenance on the track was done immediately before the event, which may have reduced the lateral strength of the rail [30].

The problem of hunting stability was one of the most fundamentals to the development of high-speed rail. Several studies of this problem were presented in the following years, it was even done a contest to solve it by UIC. Some of the answers were not widely known and some were even contradictory. More robust research into high-speed rail paid off in the end of the XX century, as a result of continued investment by research institutes and companies [30, 35].

2.3 In the modern era

Currently, in Europe, there is an increase in vehicle registration, mostly due to the motored vehicles, as shown in Figure 5. However, the figure also shows there are still a difficulty in the interoperability and in the registration of vehicles across the European Union [37].

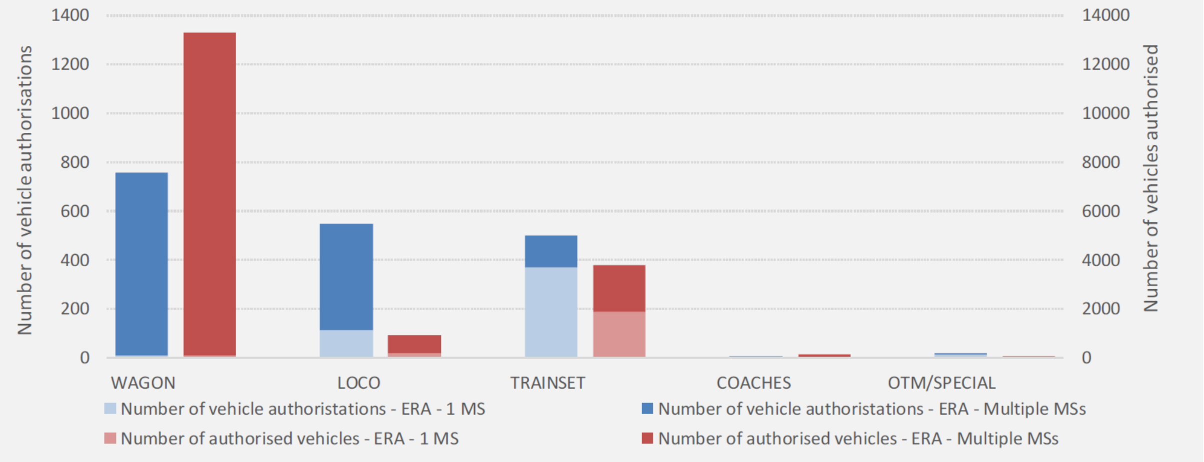

Figure 5 -Number of vehicles authorized and number of authorizations in 2022, in one or in several Member states [37].

2.3.1 *Track and loading gauges*

One of the most fundamental difference between different rail infrastructure system is the track and loading gauges; rolling stock must be design in accordance with the gauges in which will operate [20].

The track gauge is the nominal width between the two inside running faces of rails; commonly this vary from 1000 mm (metric gauge) to 1676 mm; the standard and most common gauge is 1435 mm [20].

The loading gauge defines the maximum height and width that a wagon must have in order to circulate safely on the corresponding infrastructure. It assures the maximum dimension swept by the vehicle leaves enough clearance to the surrounding structures. Loading gauges depend on the country and the specific line, for example double decker car are only able to circulate in specific section of the infrastructure. Furthermore, the difference may be the maximum height, width, or the *roundness* of the top of the reference profile. Figure 6 shows the most common loading gauge in Portugal [38].

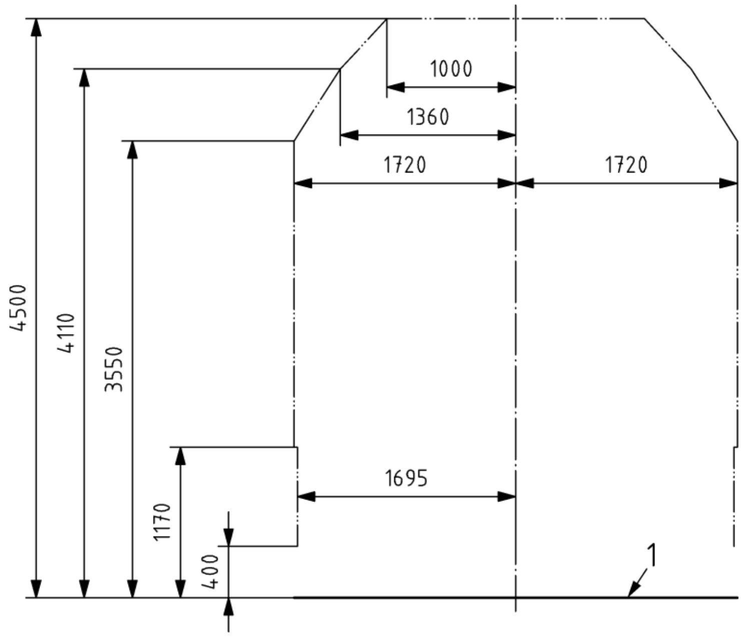

Figure 6 - Portuguese loading gauge, PTb (adapted from [38]).

2.3.2 Electrification

Currently there are several electrification standards in Europe, both in AC and DC [39]:

- 1.5 kV DC;
- 3 kV DC;
- 25 kV 50 Hz AC;
- 15 kV 16.7 Hz AC.

With regard to infrastructure on the continent, Figure 7 shows that the majority of European rail freight corridors are electrified, although with different types of electrification (shown in different colours).

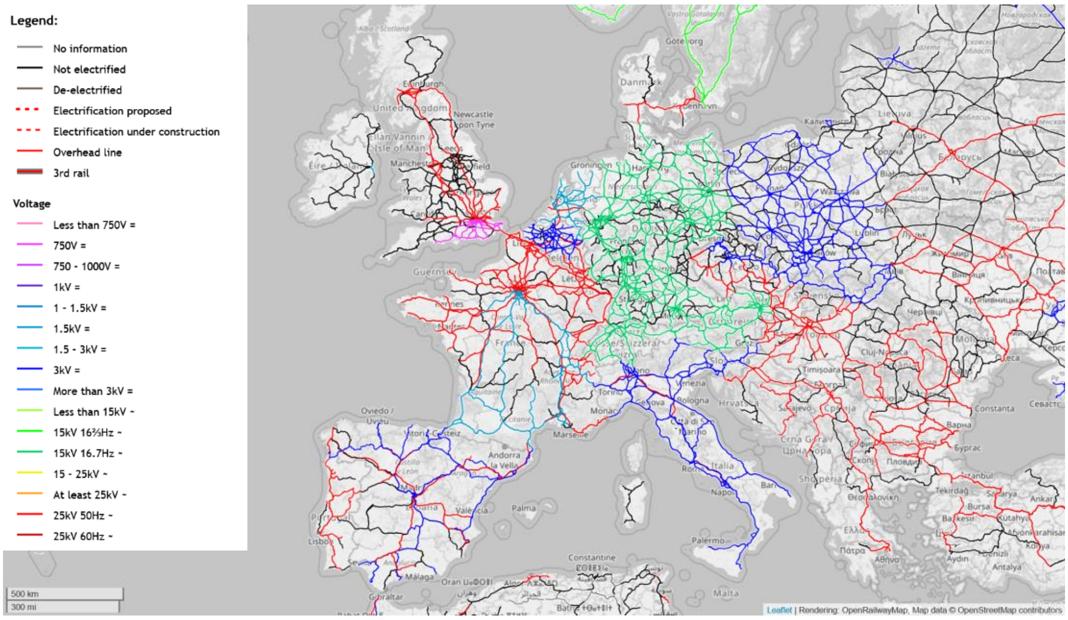

Figure 7 - Electrification of European corridors rail lines [40].

2.3.3 Railway industry in Europe

The great evolution in the technology in the turn of the millennium had great impacts in the railway industry. Looking at Europe, most of the developments was done thanks to government backed programs. The railway sector was characterised by several manufacturers, with 50 in 1980. In the last 30 years, there has been a great deal of consolidation due to merges and acquisitions, resulting in two large manufacturers (Siemens Transportation Systems, and Alstom) and several smaller, such as, CAF, Talgo and Stadler (see Figure 8). Recently, Asian companies have invested in reaching the European market, for example, the Chinese CRRC Corp. Ltd. (the biggest rail supplier) or Hitachi Rail, which acquired Ansaldo STS [30].

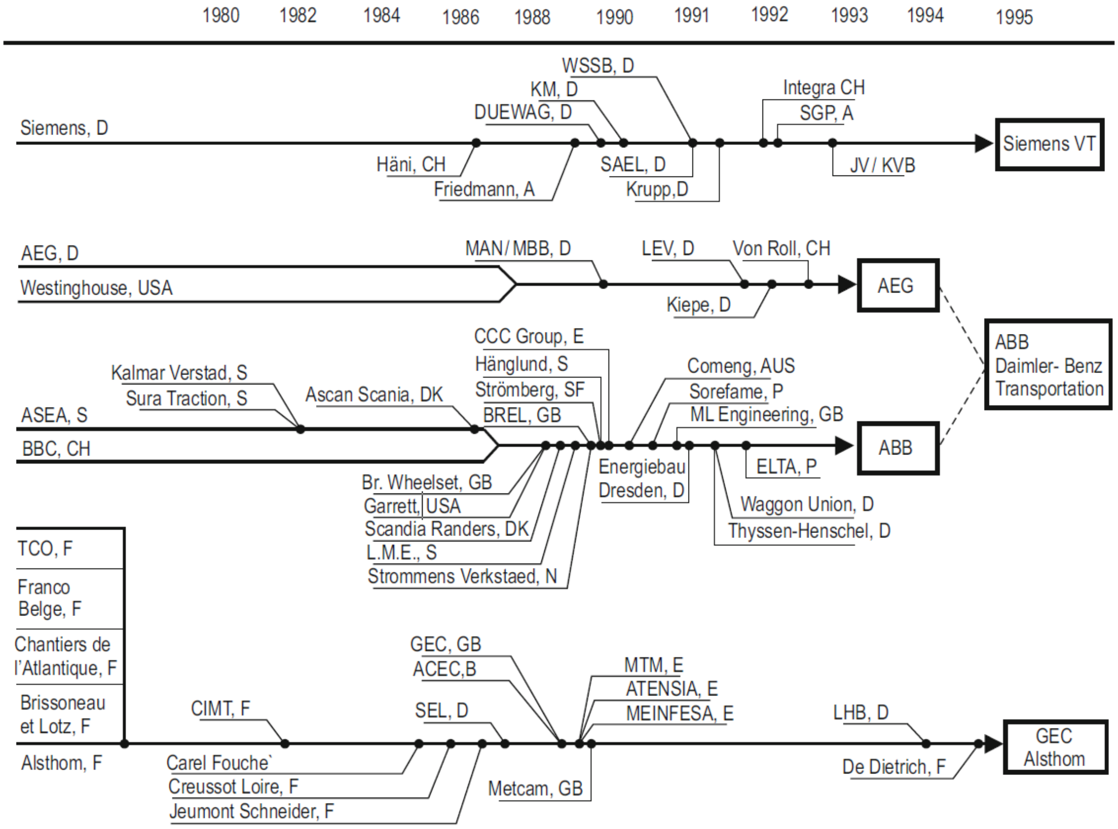

Figure 8 - Consolidation process for Central European rail vehicle manufacturers (1980-1996) [30].

2.3.4 High speed rail (HSR)

According to the High Speed Atlas [41], a High speed passenger train is able to operate at more than 200 km/h. A rail line can be considered also High speed, if it has all the necessary condition to support trains travelling above the 200 km/h. This means that it complies with the rules on operations, physical or temporal segregation with scare services and signalling [42].

The HSR was developed in Japan, due to the impossibility of upgrading an old rail line between Tokyo and Osaka. In October of 1964, the first *Shinkansen* line was opened and had a maximum speed of 210 km/h. Currently these trains are capable to reach 300 km/h in regular operation [20, 43].

In Europe, several countries invested in the development of technology to modernize the declining rail industry. The first successful service was done on 27 September 1981, between Paris and Lyon. SNCF, the French national company, was able to reach a maximum speed of 260 km/h [43].

After the success achieved by the French company, several other countries followed its example. The length and number of countries with high-speed lines has been increasing ever since. This evolution can be seen in Figure 9.

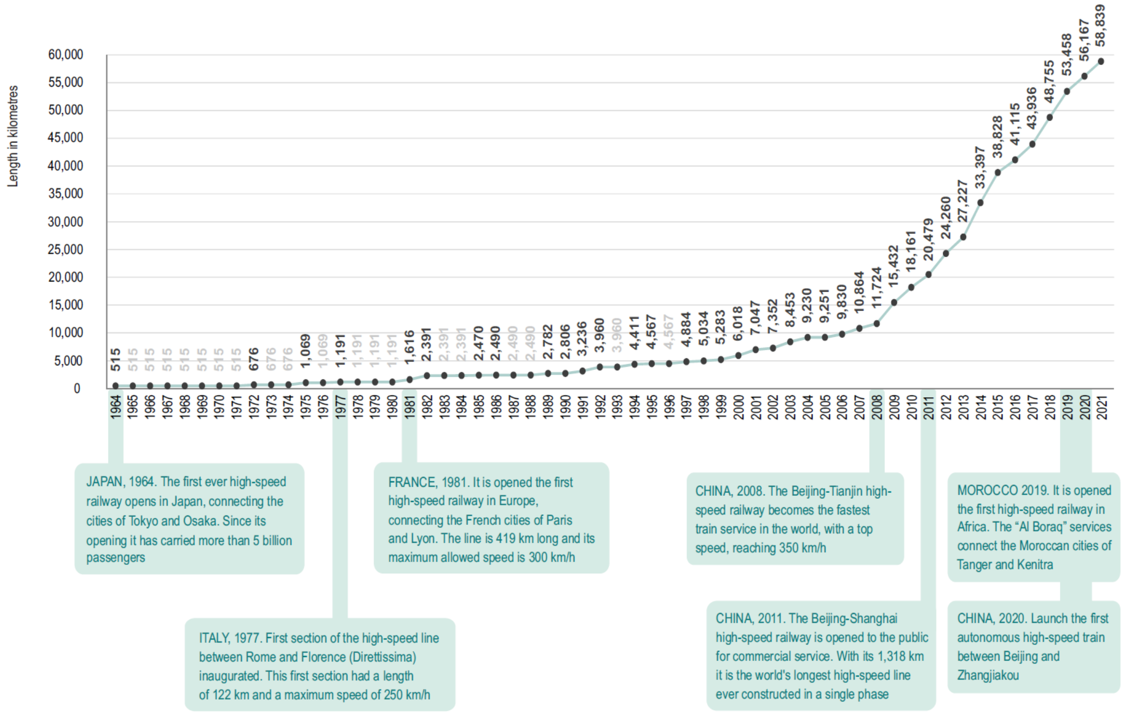

Figure 9 - Length of high-speed lines in commercial operation, in km, worldwide, by year[41].

2.3.5 Future developments

In the near future, according to UIC[44], there are four main areas for development:

- Transforming cities and connecting communities;
- Energy, technology, and innovation;
- Intermodality and the seamless connection;
- Customer experience.

In the last few years public transportation, and specially rail transportation, have gained greater popularity and see increased investment. They have been also a source of employment for several people working in the petrol industry, who became unemployed due to the energy transition [44]. This transition also includes the pursuit for greener cities and better-connected communities, one of the goals of the next decade for the industry. The modal change from cars and trucks to trains and the development of trains hubs will able the business creation and cleaner spaces in cities [44].

This transition is seen in all sectors of the economy, looking for cleaner transportation. Naturally, rail efficiency is an advantage, however, in the future there is a need to totally reduce the use of diesel which will mean innovative solution to supply areas and routes where electrification is not viable. The development of battery and hydrogen fuel cells development are necessary. Furthermore, the rail industry is looking to be an advocate of clean renewable energy sources. Besides these innovations, the development of more efficient solutions can contribute to this transition, such as, Hyperloop or Maglev, which try to increase efficiency and speed by reducing drag [44].

Finally, the aim of several developments will be the customer experience and the interaction between the railway industry and society. The development of stations thought for all people will be fundamental for this role. The improvement of rail experience will also come with the creation of new tickets and services, such as season passes or the new generation of night trains [44].

2.4 Railway in Portugal

The development of the railway in Portugal began in 1845, when the Portuguese state signed a contract with the *Companhia Real dos Caminhos de Ferro Portugueses*, which was a privately owned company (mainly foreign capital), which was the main executor of the railway development in Portugal. The first railway line was inaugurated on 28 August 1856 and, when completed, connected Porto to Lisbon in 1877, becoming the first land link between these cities. In the turn of XX century, Portugal would see a great development of the rail network, which stagnated in 1920, reaching its maximum length in 1950. Figure 10 shows the network length evolution until 2020 [5, 45].

The first rail constructions were done using the English gauge, the current standard gauge of 1450 mm. However, in 1865 it was decided to switch to the Spanish 1668 mm gauge, in line with the neighbouring Spanish network [5, 45].

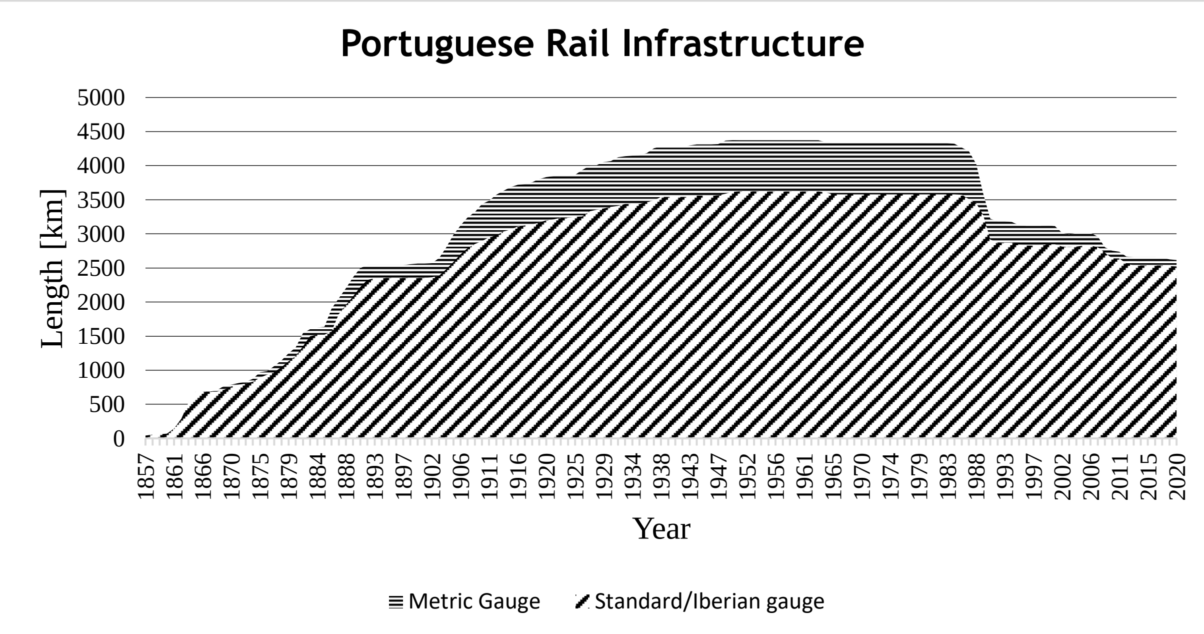

Figure 10 - Length of the Portuguese rail network, with the track gauge along the years [5]

As can be seen in Figure 10, the railway network stagnated until 1965. Subsequently, with the emergence of other modes of transport, the length of the network was reduced until today, with the closure of lines with less traffic. Until 2005, most of the metric gauge lines were closed, as well as several others with Iberian gauge. After 2005, some of the lines were reopened for freight trains. On the other hand, it was during this period that the main lines were doubled or quadrupled in some cases. There are currently 2,527 kilometres of track [5].

The first electrified line was built between Lisboa and Cascais, in 1926, with an electrification of 1.5 kV DC being adopted. The next investment was done in 1957, in lines around Lisboa. This time the the European standard of 25 kV AC was selected, with frequency of 50 Hz. Nowadays, still several lines are not electrified, although, 70% of the operated rail lines are electrified [45, 46].

Regarding the production of rolling stock, the industry in Portugal started with a partnership between *Sorefame* (*Sociedades Reunidas de Fabricações Metálicas, S. A. R. L.*) and the American rolling stock manufacturer BUDD Company. *Sorefame* bought the production rights and was able to form its workers for the railway industry. Many of production of *Sorefame* was done in partnership with other bigger manufacturers. In 1994, *Sorefame* was acquired by ABB, which afterwards was merged with Daimler Benz, forming *AdTranz*. In this scenario, the Portuguese unit was leader in innovation and automation. However, in the turn of the century, the consolidation of the industry, the increased standardizations of the sector (which required less local customization) and poor capacity of the factory to optimize local supply chains, resulted in the salle of the unit to Bombardier. After the transaction the Portuguese market dwindled, leading to the closure of the factory in 2004 [47].

In the 1990s, CP founded EMEF with the aim of renovating rolling stock to supply the demand for rolling stock, reaching an agreement with Siemens to reach this aim. In 2019, EMEF was integrated with CP in order to renovate the company's fleet [48].

2.5 The modern passenger car design

A railway vehicle can be classified in various ways, the main categories are passenger or freight wagons. Considering the objective of this thesis, it will be analysed with more focus the passenger car specifications and most relevant design decisions. Although passenger vehicles can be motorised, as is the case with multiple units, only unpowered cars will be considered. In addition, a passenger railway vehicle can be divided into two parts: the car body structure; and the bogie. Some main dimensions and characteristics must be defined for the car body as a whole [29]:

- Number of axles, the number of wheelsets supporting the structures, which in the case of passenger cars are connected in bogies;
- Vehicle wheelbase, the longitudinal distance between the outer bogies centre;
- Length between coupler axis, the longitudinal space taken by the car when connected with another;
- Length of cantilever part, half the difference between the length between coupler axis and vehicle will base;
- Car body length; the maximum length of the car;
- Coupler hight, measured from the rail top level, will vary depending on the load in operation, but has maximum and minimum values set by regulators, to ensure the coupling safety;
- Clearance diagram, which define the cross-section dimensions, important to determine the acceptance of the rail car depending on the loading gauge.

In the case of rail passenger transport, carriages are classified according to their interior layout. Examples are restaurant carriages, hostess carriages and sleeper carriages, and there may be other categories such as double-decker carriages.

2.5.1 Car body

The car body is the structure responsible for joining all the parts of the railway vehicle and the one that determines the type of vehicle, as well as the place where the vehicle's registration number is placed. The car body is connected to the bogies [29, 49].

The design must consider the necessary stiffness of the structure, and the capability of withstanding the maximum external loads it will be subjected to, in operations. Finite element method (FEM) is used to ensure the structure compliance of these requirements. Safety requirements should also be ensured, and crashworthiness analysis should be done. One feature present in passenger coaches for this reason are anti-climb devices, to ensure, in case of derailment, the coach does not rise and push the next coach. Another design requisite is related to the capacity of the structure to dissipate energy in the case of a frontal collision. This can be done either by creating plastic deformation in a controlled manner or by passing the energy on to the other trains. To evaluate this requisite crash energy management (CEM) techniques are used [29, 49].

The non-structural elements divide the carriage into 3 sections: i) under the roof, where the air conditioning systems and water tanks are located; ii) the central part, where all the equipment is located; and iii) the lower part (under the floor), where the power generator, batteries, used water and all the necessary equipment are located. These sections is supported by the frame and can be open or closed.

In terms of the structural elements several structural solutions have been used:

- Reenforced metal sheets;
- Carcass systems;
- Panel systems.

In the case of Reinforced Metal Sheets, these are made up of metal sheets that support the loads and the reinforcement is intended to increase stiffness. A solution to improve buckling resistance, sometimes, corrugated sheets are used. The joints of the structure can either be rivets or welded. This solution can lead to a low bending vibration frequency (around 8 Hz), which during operation can lead to worst comfort characteristics.

In the case of carcass systems, the metal beams are the bearing structural elements, and the external sheets have a more visual function, although, these can also improve the stiffness behaviour. Thus, these sheet materials can be other than steel, such as, plastics or light alloys. Considering, that the same coach can have different beam profiles and a complicated disposition, this solution has a high manufacturing cost.

Finally, a panels system can also be used, consisting of a set of internal and external walls, made of extruded aluminium profiles, jointed together. This process can be done by several solutions, for example, honeycomb structure or polyurethane foam. The main advantages of this are the high strength, low cost, and ability to absorb vibrations.

2.5.2 Bogie

Bogies are structures connected to the body that contain the railcar wheelset. These have several structural and stability purposes [50]:

- Support the railcar;
- Assure the running stability along strength and curved tracks;
- Absorb the vibrations produced by rail irregularities and reduce the impact of curves' centrifugal forces, guaranteeing a suitable ride comfort;
- Attempt to minimize the appearance of track irregularities.

Only non-motorised bogies will be considered, given the scope of this work.

2.5.2.1 Type of bogies

Classifying bogies can be done by several criteria: number of axes, the design, and the structure of the suspension. Since the track has 2 rails, each axle is composed by two wheels, a bogie can differ in the number of axes. The most common type is 2-axis bogie, since has a much better performance than a single axes bogie, which transmits the irregularities to the car body or the 3-axis bogie, which has reduced strength in the frame, higher complexity, and poor running performance [29, 50].

Regarding the connection to the car body, there are non-articulated bogies, more common, in cases where one car body is supported by 2 bogies and non-articulated bogies, where each bogie supports two rail cars, acting as the articulation. Although more complicated and higher maintenance, articulated bogies have increased comfort, since there is no hover hanging sections and the passenger do not ride over the bogie [29, 50].

The most relevant criteria are the definition of the bogie structure, which can be an oscillating suspension bogie or a small bogie with a lateral reinforcement spring, illustrated in Figure 11.

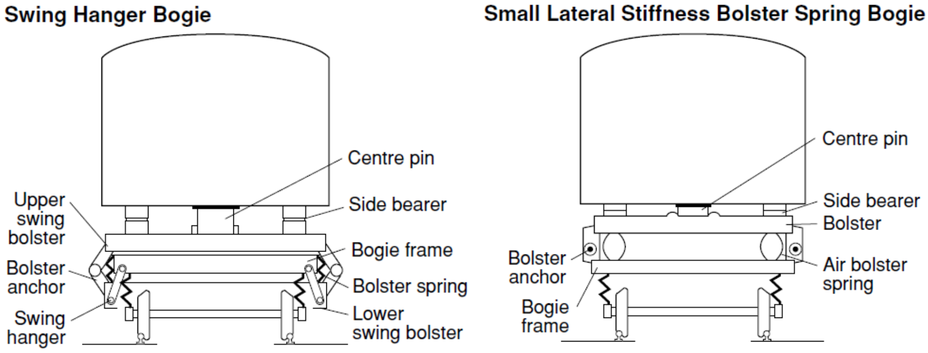

Figure 11 – Type o Bogie design, depending on the Bolster type [50].

Another important bogie differentiation is the existence of a bolster in the structure. The difference between these two options lies in the mechanics related to the rotation and control of the hunting movement. First appeared the bolster bogies, where rotation is done with a central pivot and side bearers that prevent rotation. In this case the bolter is connected to the car body by the secondary suspension and rotation is done between the bolster and the bogie structure. Later, were developed bolsterless bogies where the rotation is controlled by the secondary suspension springs [49, 50].

2.5.2.2 *Suspension*

There are several elements in the bogie with specific purposes, as the suspensions that are one of the most important features and have several variations. This is divided into 2, the primary suspension and secondary suspension. This first is located between the wheelset or axle guide and the bogie frame and is responsible for reducing the loads caused by track irregularities from being transmitted to the bogie structure. The secondary suspension has several configurations and is responsible for absorbing the vibration that will negatively affect the passenger comfort [29, 50].

Besides these components, the axle guide is a relevant component, which has several possible configurations. This component is responsible for connecting the wheel axle to the remaining bogie. In Figure 12 can be seen the several option that have been employed in current models [50].

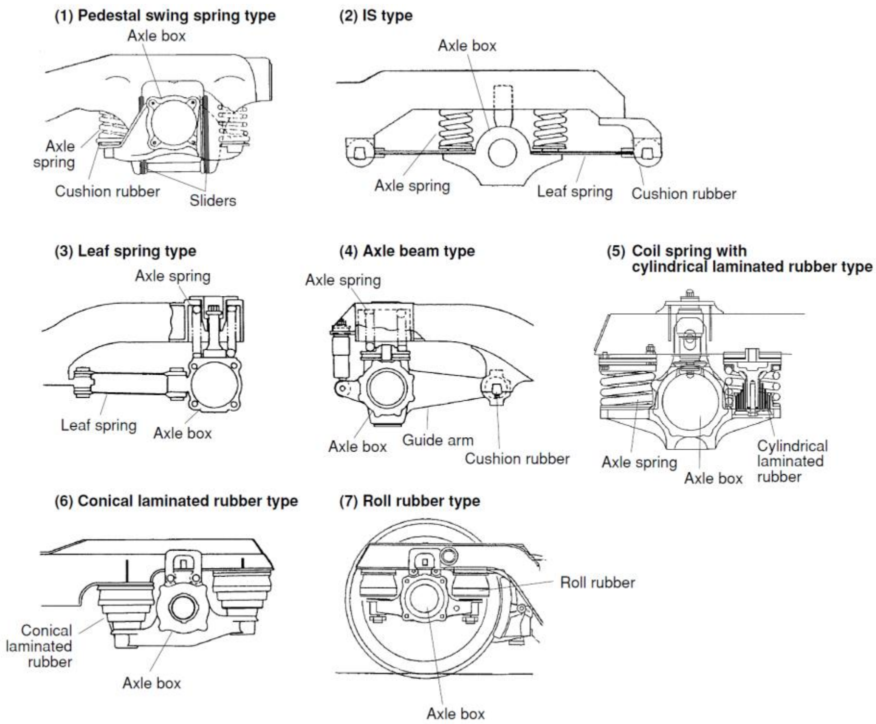

Figure 12 - Types of Axle Guide design [50]

2.5.2.3 Wheelset

Finally, the contact with the rail is done by the wheels. The wheelset comprises two wheels connected by an axle and has several functions: i) ensuring the correct distance between the wheels, transmitting the braking and acceleration forces to the rails; and ii) ensuring the wagon's orientation on the track. This are usually solid structure, although, in the 1950s were tried hollow shapes, which were abandoned to the reduction of the bending strength [49, 50].

2.6 Standards and regulations for railway passenger design

In the design of a railway passenger car is fundamental the fulfilment the necessary regulations. An overview will be given on the standards and regulations relevant to mechanical design, as well as a more detailed description of those most relevant to the multi-body dynamics of railway vehicles, which are considered in section 5.1.

2.6.1 Technical specifications for interoperability (TSI)

TSI [39] are the main rules that manufacturers must comply with in order to certify railway cars. A European testing and design standard is associated with each requirement.

The most relevant for the structural design are:

- EN 14363, for the dynamic behaviour and derailment test requirements;
- EN 12663, which defines the load requirements of the structure;
- EN 15273, define the limit dimensions due to the track gauges;
- EN 13749, for the structural requirements for the design of the bogie;
- EN 15227, which defines the crashworthiness requirements.

2.6.2 EN 14363 [51]

Standard EN 14363 - Railway applications - Testing and Simulation for the acceptance of running characteristics of railway vehicles - Tests of running and stopping behaviour [51] establishes the tests needed to guarantee the safety of railway vehicles. Different stages of testing are set: i) the first aims to assess the wagon's safety against derailment on a twisted track; while ii) the second has a broader scope and assesses dynamic behaviour on different track layouts. For the mass considered, the loading and unloading behaviour must also be assessed in accordance with EN 15663.

2.6.2.1 Safety against derailment in twisted track

This standard proposes three methods for testing such limit states, setting different conditions and tracks to evaluate derailment, and analyses different properties. The common condition is the curved track layout. However, in method 1 the track is canted (the rails have different heights) and in method 3 there is no transition between the linear and curved sections.

Focusing on Test method 1. This method using the wheel lift of the outer wheel in the leading wheelset. The criteria limit is $\Delta z \leq 5$ mm. The track is defined by a curve, with curve transition with a radius of 150 m. This test considers an initial rail cant positive on the outer rail, which has a twist, i.e., goes from a positive to a negative cant.

The dimension of the twist is $2a$, which will also define its inclination. This test can evaluate both the bogie twist and rail car twist:

For bogie twist test $2a = 2a^+$, the wheelbase of the bogie and the maximum twist inclination g^+_{lim} in ‰ is given by:

$$g^+_{lim} = \begin{cases} 7, & 2a^+ \leq 4 \text{ m} \\ \dfrac{20}{2a^+} + 2, & 2a^+ > 4 \text{ m} \end{cases} \tag{2.1}$$

When testing the car body twist, $2a = 2a^*$, the distance between centre pivots and the maximum twist inclination g^*_{lim} in ‰ is given by:

$$g^+_{lim} = \begin{cases} 7, & 2a^* \leq 4 \text{ m} \\ \dfrac{20}{2a^*} + 2, & 4 \text{ m} < 2a^* \leq 20 \text{ m} \\ 3, & 20 \text{ m} < 2a^* \leq 30 \text{ m} \\ \dfrac{90}{2a^*}, & 2a^* > 30 \text{ m} \end{cases} \tag{2.2}$$

In bogie vehicles, this test should be performed combining both.

2.6.2.2 Dynamic performance evaluation

The second part of the standard aims at evaluating the dynamic performance in different conditions. To fulfil this objective, it defines 5 types of track sections with different characteristics, as shown in Table 1.

Table 1 - Track sections definition defined by EN1463 for dynamic behaviour testing (adapted from[51])

	Test zone				
	Stability	**1**	**2**	**3**	**4**
Description	Tangent track and very large radius curves		Large radius curves	Small radius curves	Very small radius curves
Objective	Testing the vehicles running stability	Testing in the area of the vehicle's admissible speeds	Testing the combinations of the vehicle's admissible speeds and cant deficiencies	Testing around the vehicles admissible cant deficiency Including track sections with contact geometry that creates adverse steering conditions for a wheelset in test zone 4	
Anticipated vehicle dynamic behaviour	Highest probability of unstable running behaviour	There are no or only low quasi-static guiding forces or accelerations, but larger dynamic content in all assessment quantities	Superposition of quasi-static and dynamic contents of all assessment quantities	Larger quasi-static guiding forces, vertical wheel forces and accelerations, dynamic content generally decreases	
Curve radius				400 m<R<600 m	250 m<R<400 m
Test speed *V*	$V_{adm} < 100$ km/h: $V = V_{adm} + 10$ km/h 100 km/h $< V_{adm} < 300\ km/h$: $V = 1.1 \bullet V_{adm}$ $V_{adm} > 300$ km/h: $V = V_{adm} + 30$ km/h		$V_{adm} \leq V \leq 1.1 \bullet V_{adm}$	$V \leq 1.1 \bullet Vadm$	
Test cant deficiency I (evaluation range)	$I < 40$ mm		$0.70\ I_{adm} < I < 1.15\ I_{adm}$		
Length of track section		$V_{adm} \leq 160$ km/h: 100 m 160 km/h $< V_{adm} \leq 220$ km/h: 250 m $V_{adm} > 220$ km/h: 500 m		100 m	75 m

This test is meant to be performed in several track sections for each test zones. Considering that the test is carried out under railway conditions, statistical methods for interpreting the results are also defined, as well as the limit conditions for the tracks used. For this work, all the conditions will be considered exact. These may also vary in terms of the type of vehicle. For example, for passenger cars $I_{adm} = 150$ mm.

It is also relevant to understand the physical quantities relevant to determine the dynamic behaviour as well as their limit. In Table 2 can be seen all these quantities, the filters that should be applied, their purpose and its limit (when applicable). The standard also defines 200 Hz as minimum sample rate.

Table 2 - Assessment quantities and data filter according to EN 14363 for dynamic testing, where m^+ is the bogie mass and P_{F0} is the statical vertical wheelset force

Assessment quantity		Limit values	Filter
		Running safety	
Sum of guiding forces of left and right wheel	$\sum Y_{jmax}$	$k_1\ (10\ kN\ + P_{F0}/3)$ $k_1\ =\ 1.0$	Low-pass filter 20 Hz a and sliding mean method with - window length 2.0 m - step length ≤ 0.5 m
Derailment coefficient	$(Y/Q)_{j,a,max}$	0.80	
Lateral acceleration on bogie frame above axle box	$\ddot{y}^+_{j,\mathrm{max}}$	$12\ \mathrm{m/s^2}\ -(m^+\ /\ 5\ \mathrm{t})\ \cdot \mathrm{m/s^2}$	Low-pass filter 10 Hz
Lateral acceleration on vehicle body above running gear	$\ddot{y}^*_{m,S,\mathrm{max}}$	Test zone 1,2: 3.0 $\mathrm{m/s^2}$ Test zone 3: 2.8 $\mathrm{m/s^2}$ Test zone 4: 2.6 $\mathrm{m/s^2}$ c	Low-pass filter 6 Hz
Vertical acceleration on vehicle body above running gear	$\ddot{z}^*_{m,S,\mathrm{max}}$	3.0 $\mathrm{m/s^2}$ single suspension or deflated air spring: 5.0 $\mathrm{m/s^2}$	Band-pass filter 0.4 Hz to 4 Hz
		Running safety – Stability	
	$\sum Y_{j,rms}$	$k_1(10\ \mathrm{kN}\ + P_{F0}/3)/2$ $(= \Sigma Yj, max, lim\ /\ 2)$	Band-pass filter $f0 \pm\ 2$ Hz and
	$\ddot{y}^+_{j,\mathrm{rms}}$	$[12\ m/s^2 — (m^+\ /\ 5\ \mathrm{t}) \bullet m/s^2\ ]/\ 2$ $(= \ddot{y}^+_{j,\mathrm{max,lim}}\ \ /2)$	Sliding rms method with - window length 100 m - step length ≤ 10 m
		Running safety — Overturning criterion	
Overturning parameters	κ (For test conditions with $l_{adm} >$ 165 mm)	1.0	Low-pass filter 1.5 Hz

Table 2a- Assessment quantities and data filter according to EN 14363 for dynamic testing, where m^+ is the bogie mass and P_{F0} is the statical vertical wheelset force (continuation)

Assessment quantity		**Limit values**		**Filter**
		Track loading		
Quasi-static guiding force	$Y_{j,a,qst}$	60 kN		
Quasi-static vertical wheel force	$Q_{j,a,qst}$	$P_{F0} <$ 225 kN:	145 kN	
		225 kN $< P_{F0} < 250\ kN$:	155 kN	
Max. vertical wheel force	$Q_{j,a,max}$	$Test\ zones$ 1 and 2:		Low-pass filter 20 Hz
		$V_{adm} <$ 160 km/h:	MIN(90 kN + Q_0; 200 kN)	
		160 km/h $< V_{adm} \leq$ 200 km/h:	MIN(90 kN + Q_0; 190 kN)	
		200 km/h $< V_{adm} \leq$ 250 km/h:	MIN(90 kN + Q_0; 180 kN)	
		250 km/h $< V_{adm} \leq$ 300 km/h:	MIN(90 kN + Q_0; 170 kN)	
		$V_{adm} >$ 300 km/h	MIN(90 kN + Q_0; 160 kN)	
		$Test\ zones$ 3 and 4:	MIN(90 kN + Q_0; 200 kN)	
		$For\ all\ test\ zones\ with$: $V_{adm} <$ 100km/h 225 kN $< P_{F0} \leq 250\ kN$:	MIN(90 kN + Q_0; 210 kN	

2.6.3 EN 12299 [52]

The standard EN 12299 defines methods for evaluating passenger ride comfort in railway, due to vibration. Although, other standards were available to evaluate human response to vibration, these were not accurate or adapted to the type of vibrations experienced in rail transport, such as ISO 2631. These standards focused on mean vibration, disregarding significant singular vibrations. Due to this, the EN12299 is developed in order to assess these factors, each is defined by a different reference value[30]:

- Mean and continuous comfort;
- Comfort on curve transition;
- Comfort on discrete events.

2.6.3.1 Mean and continuous comfort

The Mean comfort is evaluated using N_{MV}, obtained from the acceleration determined in ISO 2631. In the international standard, an effective acceleration is determined according to Eq. (2.3). Different frequencies will have different impact on the comfort felt by humans.

$$a_{\text{eff,ISO}} = \sqrt{\frac{1}{T}\int_0^T a_{\text{ISO}}^2(t)dt} \tag{2.3}$$

Where:

- $a_{\text{eff,ISO}}$ is the effective acceleration value for a period of T,

- $a_{\mathrm{ISO,i}}$ is the instantaneous acceleration, adjusted by the weighting filter,
- T is the period of the interval.

The weighting function applied to the acceleration will depend on the direction and applied after applying to the measured acceleration low-pass and high pass filters. Figure 13 shows the weighting curves and Table 3 shows the application of each one and the corresponding filters:

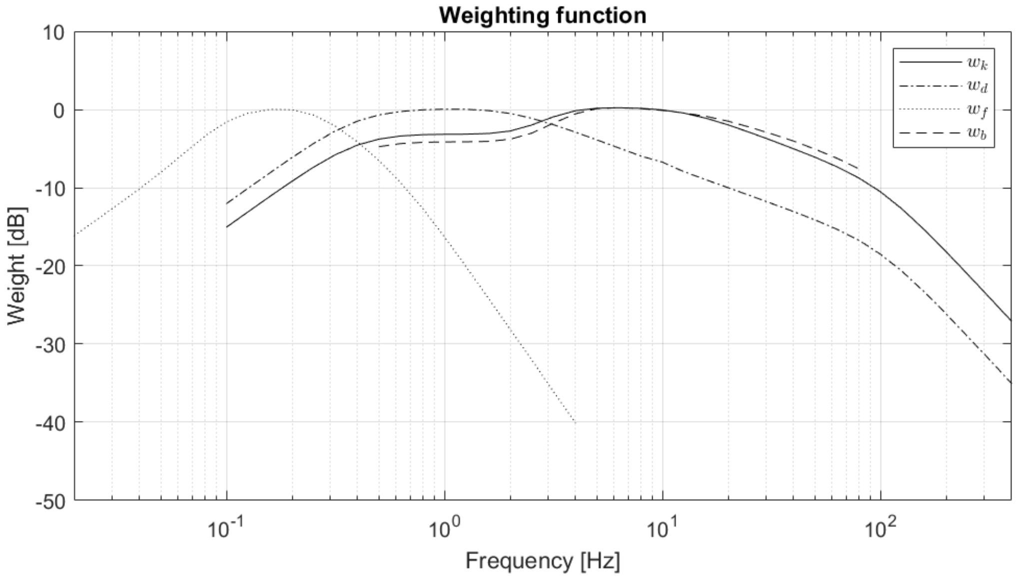

Figure 13 - Weighting curves according to ISO 2631 [53], in dB depending on the frequency in Hz.

Table 3 - Weighting curves defined in ISO 2631 [54] applicable in different direction and band of frequencies

Weighting curve	Direction	Filtered frequencies
$\boldsymbol{w_k}$ or $\boldsymbol{w_b}$	Vertical	0.5 Hz – 80 Hz
$\boldsymbol{w_d}$	Transverse and longitudinal	0.5 Hz – 80 Hz
$\boldsymbol{w_f}$	Vertical	0.01 Hz – 0.5 Hz

In the case of rail applications, w_k is substituted by w_b and in this case w_f is not applied. For the rail vehicles, the accelerations are measured in the centre of the car body and above the bogie, on the floor level. Afterwards, the effective acceleration is calculated, which must be calculated for at least 60 consecutive 5-second intervals in the 3 directions, as shown in Eq. (2.4) [54]:

$$a_{\mathrm{eff,ISO,i}} = \sqrt{\frac{1}{5}\int_{5(i-1)}^{5(i)} a_{\mathrm{ISO,i}}^2(t)dt} \qquad i = 1,60 \tag{2.4}$$

For each direction is considered the 95 percentiles of the 60 values for the calculation of N_{MV}

$$N_{\mathrm{MV}} = 6 \cdot \sqrt{\left(a_{\mathrm{x95,wd}}\right)^2 + \left(a_{\mathrm{y95,wd}}\right)^2 + \left(a_{\mathrm{z95,wb}}\right)^2} \tag{2.5}$$

This value will determine the level of comfort as shown in Table 4.

Table 4 - Equivalence between N_{MV} and the level of ride comfort according to EN 12299 [52]

$\boldsymbol{N_{\mathbf{MV}} < 1}$	Very comfortable
$\mathbf{1} \le \boldsymbol{N_{\mathbf{MV}}} < \mathbf{2}$	Comfortable
$\mathbf{2} \le \boldsymbol{N_{\mathbf{MV}}} < \mathbf{4}$	Medium
$\mathbf{4} \le \boldsymbol{N_{\mathbf{MV}}} < \mathbf{5}$	Uncomfortable
$\boldsymbol{N_{\mathbf{MV}}} \ge \mathbf{5}$	Very uncomfortable

2.6.3.2 Comfort on curve transition and Comfort on discrete events

Curve transition are critical locations where additional discomfort will be felt by passengers. For that reason, EN 12299 defines *Percentage disturbed from curve transition* (P_{CT}). Additionally, discrete events such as rail crossings will have an impact on passenger ride comfort, the standard defines *Percentage disturbed from discrete event* (P_{DE}). P_{CT} is defined by Eq. (2.6), where the component inside parenthesis is only considered if positive[30].

$$P_{CT} = (A\,\ddot{y}_{max} + B\,\dddot{y}_{max} - C) + D\,\dot{\varphi}^{E}_{x,max} \quad [\%] \tag{2.6}$$

where:

- $\ddot{y}_{max}$ is the maximum lateral acceleration, considering the interval between the beginning of the curve transition and 1.6 s after its end;
- $\dddot{y}_{max}$ is the maximum lateral jerk, considering the interval between 1 s before the begging of the curve transition and its end;
- $\dot{\varphi}^{E}_{max}$ is the maximum absolute roll speed, during the curve transition.

P_{DE} is defined by Eq. (2.7).

$$P_{DE} = a\,\ddot{y}_p + b\,\ddot{y}_{\text{mean}} - c \quad [\%] \tag{2.7}$$

where:

- $\ddot{y}$ is the lateral speed;
- $\ddot{y}_p = \ddot{y}_{max} - \ddot{y}_{min}$;
- $\ddot{y}_{\text{mean}}$ is the mean value in the same interval.

For the calculation of P_{DE} the signal should be filtered by a sliding time interval of 2 s and by the w_d filter defined in ISO 2631. The constants for both equations can be seen in Table 5 and Table 6, respectively.

Table 5 - Constants value for calculation of P_{CT} [30]

Passenger	A	B	C	D	E
Standing	28.54	20.69	11.1	0.185	2.283
Seating	8.97	9.68	5.9	0.12	1.626

Table 6 - Constants value for calculation of P_{DE} [30]

Passenger	a	b	c
Standing	16.62	27.01	37
Sitting	8.46	13.05	21.7

2.7 Summary of the Chapter

As seen in this chapter, the railway industry has been evolving with different paces throughout its history. The golden age of rail development in the turn of the 20th century allows for a great increase in infrastructure, especially in Europe. After that time investment dwindled until the 1970s with the appearance of high-speed rail. The development of this technology boosted once again investment in railway. The rail industry has also evolved in recent years, with a great consolidation. In the near future, can be predicted an increase in the level of investment by both public and private enterprises.

The rich history in railway development, also led to a great variability in rail infrastructure standards. Although there has been a great effort from the EU to harmonize rail standards across the continent, there are still different track gauges, structural gauges, and electrification, depending on the country.

Currently, there are several options regarding passenger rail cars design. The car body can have different configurations and structure and the rail car can be designed for several purposes. Bogies have also great variability in their design, which will influence the dynamic performance and characteristics of the rail car.

An important step of this design is an extensive evaluation of the rail car dynamic behaviour, structural capabilities, and ride comfort. The dynamic behaviour can be evaluated according to the European standard EN 14363, proposed by the TSI, which defines two types of tests. The comfort is evaluated by EN 12299.

Once analysed the relevant standards and principles of design for rail cars, it is relevant to understand the basic principles behind multi-body dynamics and the relevant models for defining the structure.

3 Multi-body Dynamics applied to Rail vehicles

Multi-body Dynamics is a field of mechanical computation focused on the solution of nonlinear equation that govern the relation between several bodies and structure of mechanical system. These elements may be subjected to large displacements and rotations, which may be constrained by joints or connections.

Rail vehicle dynamic have a fundamental role in the design of rail passenger vehicles, providing data regarding several running characteristics of the train. Several safety and comfort characteristics must be ensured. The rail vehicle must not derail or roll over, and acceleration to which passengers are subjected must be controlled and the noise created must not exceed the defined limits. In the long term, safety must be ensured during the lifetime of the vehicle, determining behaviour along its lifetime will allow better fatigue prediction.

3.1 Dynamic formulation

In order to describe a dynamic system, there are various formulation possible. The Newton-Euler equations describe the system by using 3 translational equations and 3 rotational equations associated with each body. This are [49]:

$$\begin{cases} m_i \mathbf{a}_i = \mathbf{F}_i \\ J_i \ddot{\boldsymbol{\theta}}_\mathbf{i} = \mathbf{M}_i \end{cases} \tag{3.1}$$

where,

- m_i is the total mass of the rigid body;
- $\mathbf{a_i}$ is the vector of the acceleration of the body mass centre;
- $\mathbf{F_i}$ is the vector of forces acting on the body mass centre;
- J_i is the mass moment of inertia defined with respect to the mass centre;
- $\ddot{\boldsymbol{\theta}}_{\boldsymbol{i}}$ is the vector of the angular acceleration of the body mass centre;
- $\mathbf{M_i}$ is the moment acting on the body.

An alternative to this formulation is D'Alembert principle, which uses the principle of virtual work to determine the system equilibrium. The principle can be described by [49]:

$$\delta W = \sum_{i=1}^{n} (\mathbf{F}_i - m_i \mathbf{a}_i) \cdot \delta \mathbf{r}_i = 0 \tag{3.2}$$

From this formulation, can be used the kinetic and potential energy to determine the system equations, instead of forces, which is much simpler considering that energy is scalar instead of vectorial. This technique will result in the Lagrange equations. Another possible technique is called the augmented formulation and can be applied to formulate the dynamic equations of constrained multibody systems.

Finally, the set of second order differential equations can be written in the matrix form as [29]:

$$[\mathbf{M}]\ddot{\mathbf{q}} + [\mathbf{C}]\dot{\mathbf{q}} + [\mathbf{K}]\mathbf{q} = \mathbf{F} \tag{3.3}$$

where:

- $[\mathbf{M}]$ is the masse matrix;
- $[\mathbf{C}]$ is damping matrix;
- $[\mathbf{K}]$ is stiffness matrix;
- $\mathbf{q}$ is the system degrees of freedom generalized coordinates;
- $\mathbf{F}$ is input force vector.

3.2 Equations solver

For each model or problem different sets of equations will be defined using the approach mentioned in section 3.1. In order to obtain results, this system of equations must be solved. Depending on the intended result or data, different approaches may be necessary.

3.2.1 Eigen behaviour

The vibration of a system will consist in an alternating oscillatory movement, which occur due to the transformation of energy between potential and kinematic energy, which will occur due to the existence of mass and stiffness in the system. The response of the system only to an initial perturbation is called natural response. Such a response can be obtained from the equation of motion by calculating its eigenvalues and eigenvectors, representing the natural frequencies of vibration and the corresponding natural mode shapes of vibration. This analysis allows for the determination of the critical speed of the vehicle, by analysing the stability of each mode at several speeds. Due to the existence of creep forces in the rail-wheel contact, this will depend on the speed [29, 49, 55].

3.2.2 Quasi-static solution

This form of analysis is not common and aims to analyse the behaviour of a rail vehicle when negotiating a curve with constant radius and at constant speed. In these situations, the vehicle, after a transient period, will have a steady movement. This method will analyse the track train interaction, in this case is not possible to introduce track irregularities [29].

3.2.3 Stochastic analysis

In this type of analysis, the input is defined in statistical way. Track irregularities, both in vertical and lateral direction, as well as cant deficiency or track widening are defined by spectrum. This means the functions define an amplitude for each frequency of irregularity [29, 49].

Stochastic analyses are useful to determine the vehicle behaviour in a particular type of track. It facilitates the comparison between different vehicles. This is also useful to determine the ride comfort characteristics of the vehicle. However, this analysis requires linear equation of motion and cannot determine the response to a particular irregularity [29].

3.2.4 Time-stepping integration

The most relevant method of simulating dynamic systems is the time-stepping integration. This method obtains a solution by solving the equations of motion for each time step. There are several formulations to obtain this result numerically. The time step is a particularly relevant parameter in this analysis. Small time steps require higher computational power, but large time steps may lead to unstable solutions. There are also algorithms that vary the time step according to the situation. At each time step, the values for acceleration, velocity, position, and force can be obtained. The biggest advantage of this method is the capacity of handling non-linearities, such as, nonlinear damping or stiffness functions or spring-damper in series [29].

3.3 Elements modelling

Element modulation is crucial for a correct elaboration of a model. Too simplified elements will result in simpler models, but may lead to results that do not correspond to the original vehicle [56].

Elements are usually of two types:

- Point to Point (PtP), which calculations are done in the line of action of the element, i.e., in the line that connect the two markers of the element;
- Compact Force (Cmp), which are defined in the reference system of one of the markers.

The following type of elements will be the most relevant for the development of the model of this dissertation.

3.3.1 Coil springs

Springs are elastic elements that store energy when they are deformed and release the same amount of energy when they are released. This means that springs force will only depend on its deformations, the relation between the two properties is called stiffness [29]. There are various types of springs. In this case, only coil springs will be analysed [56].

A simplified model of a coil spring considers only the axial direction. However, in many applications the behaviour along other directions, the coupling of different directions and the influence that vertical loads not applied in the axial direction might have may have relevant impact on the result. Furthermore, some compressive preloads might cause instability in the spring, requiring the consideration of buckling effects [56].

Most coil springs in railway application have a behaviour, which does not depend on the frequency and its damping may be neglected [56].

The European standard EN 13906-1 defines several methods to determine the stiffness properties of the coil spring. Besides the axial stiffness, the standard also proposes a definition for the shear stiffness, however, it also notes that this is only constant for small deformations [57].The axial spring force can be defined, as follows:

$$F = \frac{G \cdot d^4 \cdot (L_0 - L)}{8 \cdot n \cdot D^3} \tag{3.4}$$

where:

- D is the mean coil diameter;
- d is the wire diameter;
- n is the number of active coils;
- G is the shear modulus;
- L_0 is the unloaded spring length.

This is not enough to define springs when shear and bending behaviour is relevant. Figure 14 shows the load that a spring is subjected to.

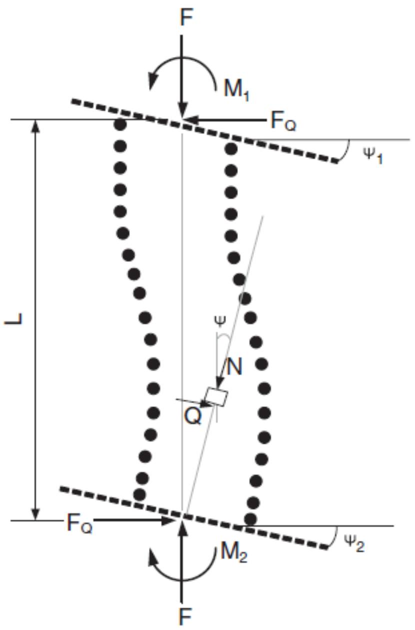

Figure 14 - Spring diagram, subject to axial load, F, shear load, F_Q and bending moments, M_1 and M_2 [56].

Krettek and Sobczak [58] developed a model to describe this spring behaviour, defining the shear stiffness, K_y^* and bending stiffness, K_ψ^*:

$$K_y^* = a_1 K_y = a_1 \cdot \left(\frac{F}{2/c\left(1 + F/R_Q'\right) \cdot \tan\,(cL/2) - L}\right) \tag{3.5}$$

$$K_\psi^* = a_3 K_\psi = a_3 \cdot \left(K_y \cdot \frac{R_\psi'}{F}\left[\left(1 + \frac{F}{R_Q'}\right) - \frac{cL}{\tan\,(cL)}\right]\right) \tag{3.6}$$

The contribution of the bending angle to the shear force and the contribution of the shear displacement to the bending force is defined as:

$$K_{y\psi}^* = a_2 K_{y\psi} = a_2 \cdot \left(K_y \cdot \frac{cR_\psi'}{F} \tan\left(\frac{cL}{2}\right)\right) \tag{3.7}$$

In these expressions a_i are correction factors in order to incorporate the buckling influence in the spring instability, defined as:

- $a_1 = 1.9619\xi + 0.6740$ Correction factor for lateral stiffness;
- $a_2 = 1.3822\xi + 0.6513$ Correction factor for mixed term (lateral/bending coupling);
- $a_3 = 0.8945\xi + 0.6690$ Correction factor for bending stiffness;

being:

$$\xi = \frac{s}{L_0} = \frac{L_0 - L}{L_0} \tag{3.8}$$

The stiffness calculations also require the definition of c, a factor, which relates the axial load with the bending and shear properties:

$$c^2 = \frac{F}{R_\psi'}\left(1 + \frac{F}{R_Q'}\right) \tag{3.9}$$

and:

$$R'_{\psi} = \frac{Ed^4L}{32nD(v+2)} \tag{3.10}$$

$$R'_{Q} = \frac{Gd^4L}{4nD^3}(v+1) \tag{3.11}$$

$$R' = RL = \frac{Gd^4L}{8nD^3} \tag{3.12}$$

3.3.2 Hydraulic dampers

Hydraulic dampers dissipate energy by forcing fluid from one chamber to another through a flow control valve, transforming kinetic energy into heat. The simplest damper model consists of a linear relation between the velocity and the damping force. More realistic models consider the stiffness in series due to damper components, as well as a nonlinear damping function. The most common modulation consists of the series of a damper element with a spring element, as seen in Figure 15

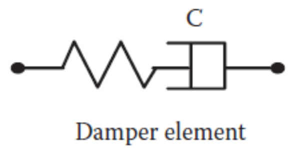

Figure 15 - Hydraulic damper model [49].

The stiffness is originated by elements such as the rubber supports, but also by the fluid inside the damper. There are several models to describe both the stiffness and damping of these elements. *Wang et al [59]* defines the stiffness of the hydraulic damper as:

$$K_e = \frac{K_{\text{seat}}K_{\text{rubber}}K_{\text{oil}}}{K_{\text{seat}}K_{\text{rubber}} + K_{\text{seat}}K_{\text{oil}} + K_{\text{rubber}}K_{\text{oil}}} \tag{3.13}$$

being,

$$K_{\text{oil}} = \frac{\beta_{\text{e}}(A_{\text{act}})^2}{V_{\text{oil}}} = \begin{cases} \dfrac{\pi\beta_{\text{e}}(D^2 - d^2)}{2\left[H - H_{\text{p}} - 2|x_{\text{r}}(t)|^2\right]} & \dot{x}_{\text{r}}(t) < 0 \\ \dfrac{\pi\beta_{\text{e}}D^2}{2\left[H - H_{\text{p}} - 2|x_{\text{r}}(t)|^2\right]} & \dot{x}_{\text{r}}(t) > 0 \end{cases} \tag{3.14}$$

where,

- A_{act} piston or rod-side area (m^2);
- K_e damper comprehensive stiffness (N/m);
- $K_{oil}, K_{rubber}, K_{seat}$ stiffnesses of oil spring, rubber attachment and steel mounting seat (N/m);
- βe, instantaneous bulk modulus of oil (Pa);
- $H,\ H_g, H_p$ heights of inner tube, guide seat and piston (m);
- $x_r(t)$ actual instantaneous displacements (m).

3.3.3 Other elements

There are several other elements that can be used to design a multi-body dynamic model. Examples of those are bump stops, in which the force depends on the displacement and is characterized by having no force output until a point of displacement where there is a steep increase in the force output. Another relevant element is the bushing which is defined by a point connection with stiffness and damping in all 6 degrees of freedom [29, 49].

There are other type of elements such as traction rods and torsion bars which stiffness and damping characteristics are given by the material properties [56].

3.3.4 Rail-Wheel contact

The rail wheel contact is the most complex part of the railway multi-body dynamic model. Its definition will have several components [30]:

- Rail and wheel profiles definition;
- Creep forces determination;
- Normal contact law.

3.4 Summary of the Chapter

Broadly, multi-body dynamics a formulation used in computational tools that allows for dynamic analysis, relevant, in particular, for rail applications. The basic principle of this technique consists on defining the system of non linear equations that define the system and solving it. Depending on the proposed of the model several options are available to solve this system. The most powerful and useful technique is the time stepped integration, which shows the dynamic behaviour along the time of the simulation.

In terms of modelling the rail car several options are available. Each component has different applicable models. Simillar elements may also be modelled differently depending on their function and load case. The most broadly used elements are springs and dampers. Although there are several types of springs, only helical springs are relevant for this work, considering the studied bogie. Within the helical spring several models were developed, depending on the number of directions considered and in the linearity of the stiffness. Regarding dampers, although simpler models may be used, the most common is the use of a stiffness element in series with a damping element. Other types of elements should also be carefully modelled, as well as the rail-wheel contact.

Since the theoretical background is presented in this chapter, the next will be focused on the construction of the model in the commercial software SimPack.

4 Passenger car model

In this chapter, a model of an ARCO passenger car will be developed in SIMPACK, as well as, the data used for this purpose. It was supplied by CP the maintenance documentation of the wagon [60], including:

- The blueprints and most relevant measurements of the bogie;
- The dimensions of the springs;
- The model of the damper, which is out of production.

SimPack Rail was developed by a joint venture between the German Aerospace Centre DLR and Siemens Transport in 1993. This software allows of modelling any rail guided systems, as well as, almost any rail application [29].

4.1 ARCO passenger car

ARCO passenger cars are part of CP fleet of rolling stock. These were bought from RENFE, included in a strategy by the company to renew its rolling stock, for 1.5 M€ [61]. CP acquired 36 of 2000 series and 14 of 10000 series, needing renovation, with an estimated cost of 150 k€ each. Some have already been renewed and are circulating in *Linha do Minho* [62, 63].

Built between 1984 and 1988 by CAF and Macosa these had a 160 km/h maximum speed with bogies *Grand Confort* (GC3A) and were, initially, denominated by 10000 series. In the late 90s, these were upgraded to a maximum speed of 200 km/h, upgrading the bogies to GC3D. This led to an upgrade in the service quality, creating the new service *Arco* (which names the entire series in CP), and renamed as 2000 series [64, 65].

Figure 16 shows the configuration after the renovation carried out by CP, in 2nd class. Complementing this disposition, first class cars and mixed cars (2nd class and bar), equipped with bicycle supports were renewed. This works will be focused on the 2nd class car.

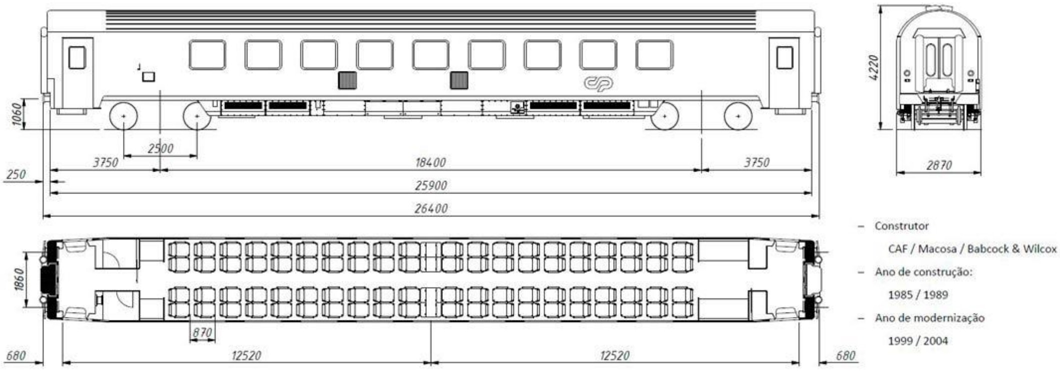

Figure 16 - Blueprint of a 2nd class CP ARCO rail car [60].

4.2 Bogie *Grand Confort* 3

All of Arco's cars have the GC3 bogie. In this work, the most modern GC3D will be considered, which allows a maximum speed of 200 km/h. From the technical documents for maintenance [66] several data can be retrieved. In this subchapter, the technical considerations and data used in subchapter 4.5.1 regarding springs and dampers, as well as the operation of all the other elements, will be explained.

4.2.1 Primary Suspension

As seen in Figure 17, the primary suspension is composed by two concentric springs and one damper. It was also considered the bearing connection between the axle guide and the main structure.

Figure 17 - Primary suspension and Axle guide of ARCO passenger cars, taken in CP workshop in Guifões.

According to [67], the spring should be modeled as a shear spring, due to the impact of bending (axle rotation), in the output force. Since the manufacture did not specify the stiffness, this will be calculated according to subsection 3.3.1 and using the data in Table 7.

Table 7 – Primary spring data defined in [66] and utilized for stiffness calculation

	Inner Spring	**Outer Spring**
D, nominal diameter	117.4 mm	193 mm
d, wire diameter	21.2 mm	34 mm
n, number of coils	7	4

The axial stiffness is constant, contrary to the bending and shear ones, which depend on the elongation. The relation between the axial, shear and bending stiffness and the deformation can be seen in Figure 18

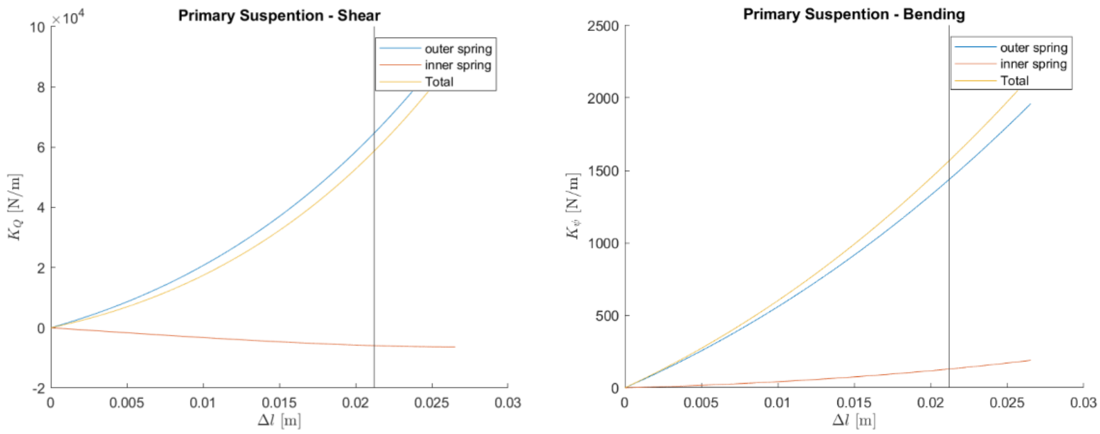

(a) (b)

Figure 18 - Variation of the shear (a) and bending (b) stiffness depending on the spring elongation, for both the inner, outer springs and the sum, with the working axial elongation (vertical black line).

The stiffness value selected as an approximation was determined by the working axial load expressed by the manufacturer as 36.75 kN, corresponding to 21.2 mm compression. The values determined can be seen in Table 8.

Table 8 - Stiffness data for the primary suspension springs, being K_z the axial stiffness, K_Q shear stiffness and K_ψ the bending stiffness

Stiffness	**Inner Spring**	**Outer Spring**	**Sum**
$\boldsymbol{K_z}$	$2.41 \cdot 10^5$ N/m	$6.24 \cdot 10^5$ N/m	$8.66 \cdot 10^5$ N/m
$\boldsymbol{K_Q}$	$-5.94 \cdot 10^4$ N/m	$6.47 \cdot 10^4$ N/m	$5.87 \cdot 10^4$ N/m
$\boldsymbol{K_\psi}$	130 N/m	$1.43 \cdot 10^3$ N/m	$1.57 \cdot 10^3$ N/m

Regarding dampers, these were modelled as described in Chapter 3, as a damping element in series with a spring (modelling the attachments). In this case, there are some information from manufacturers' catalogues [68], regarding the damper model defined in [66], which combined with literature examples [67, 69, 70], allowed the definition of the dampers' constants. As shown in Figure 19, there is an increase in the damping rate at lower speeds, at higher speeds the damping rate is equal to 8.3 kNs/m. In Table 9, can be seen the data used for the stiffness calculation, the diameters were based in manufacturer data [66], while the other data was based on the literature.

Table 10 shows the stiffness results.

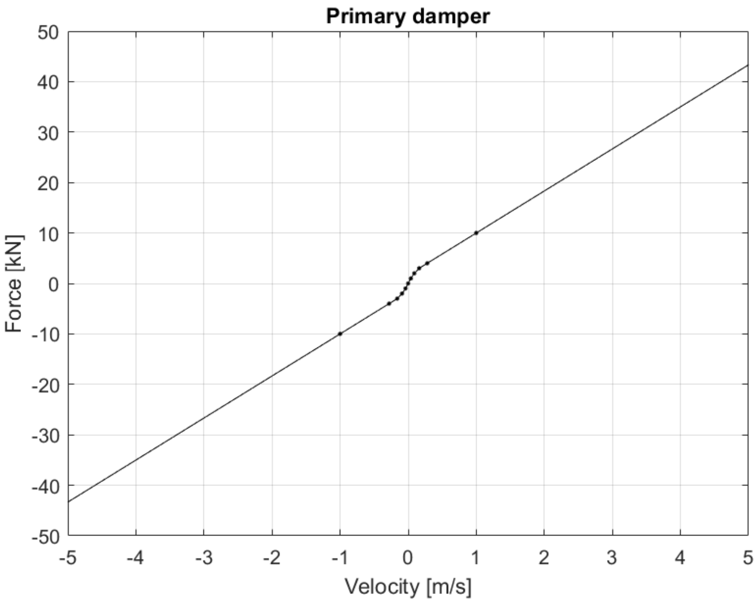

Figure 19 - Primary vertical damper, damping force [kN] by the damper speed [m/s].

Table 9 - Stiffness data for calculation of the stiffness component of the primary vertical damper [67, 69, 70]

$\boldsymbol{\beta}$	$\boldsymbol{D}$	$\boldsymbol{d}$	$\boldsymbol{h}$	$\boldsymbol{h_p}$
$1.7 \cdot 10^9$ Pa^{-1}	$100 \cdot 10^{-3}$ m	$80 \cdot 10^{-3}$ m	0.66 m	$2.5 \cdot 10^{-2}$ m

Table 10 - Stiffness of the primary vertical damper [67, 69, 70]

$\boldsymbol{K_{rubber}}$	$\boldsymbol{K_{seat}}$	$\boldsymbol{K_{oil}}$	$\boldsymbol{K_{damper}}$
$1.04 \cdot 10^6$ N/m	$1.41 \cdot 10^8$ N/m	$1.69 \cdot 10^7$ N/m	$9.73 \cdot 10^5$ N/m

4.2.2 Secondary Suspension

The secondary suspension is responsible for the connection between the main structure and the bolster. Figure 20 and Figure 21 show the longitudinal and lateral views of the bogie. It should be noted the remaining components (besides the dampers) and their function:

- Traction rod, responsible for transmitting the traction force applied to the rail car body by a locomotive to the bogie;
- Bump stop, responsible to stop the lateral displacement of the bolster in relation to the bogie structure i.e., to restrict the lateral movement of the car body;
- Anti-roll bar, meant to restrict the rotation in the longitudinal direction.

The properties of the for mentioned elements will be described in the subsection 4.5.

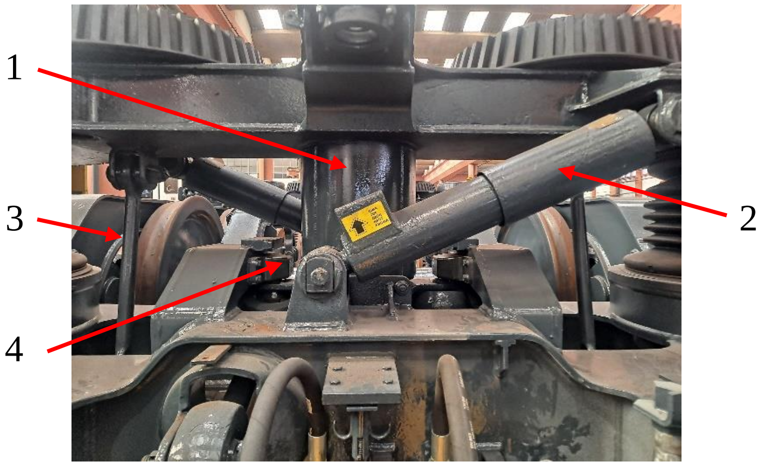

Figure 20 - Bogie GC3D longitudinal view, displaying several components: traction rod (1), transverse damper (2), anti-roll bar connection (3) and bump stop (4).

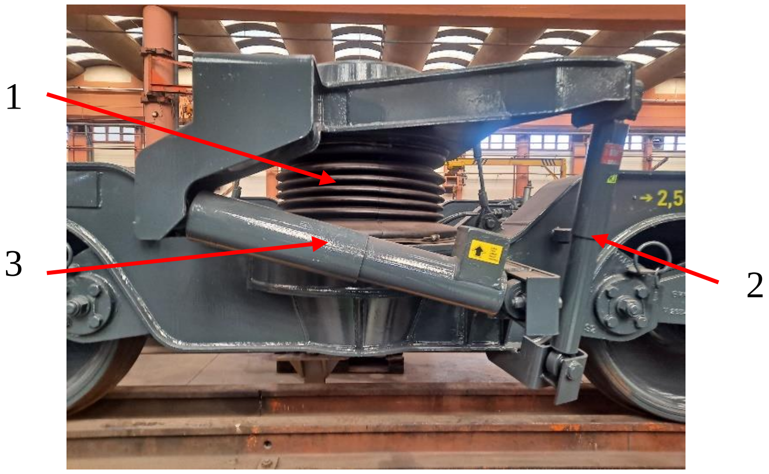

Figure 21 - Bogie side view, showing the secondary springs (1) and vertical (2) and anti-yaw (3) dampers.

The secondary springs stiffness was determined similarly to the primary spring. The secondary spring was considered a shear spring, and similarly to the primary springs, there is no data available from the manufacturer for the stiffness. The provided data is only regarding geometric dimensions and can be seen in Table 11.

Table 11 - Secondary spring data defined in [66] and utilized for stiffness calculation

$\boldsymbol{D}$	380 mm
$\boldsymbol{d}$	60 mm
$\boldsymbol{n}$	6.1

The axial stiffness is constant, contrary to the bending and shear ones, which depend on the elongation. The relation between the shear and bending stiffness and the deformation can be seen in Figure 18

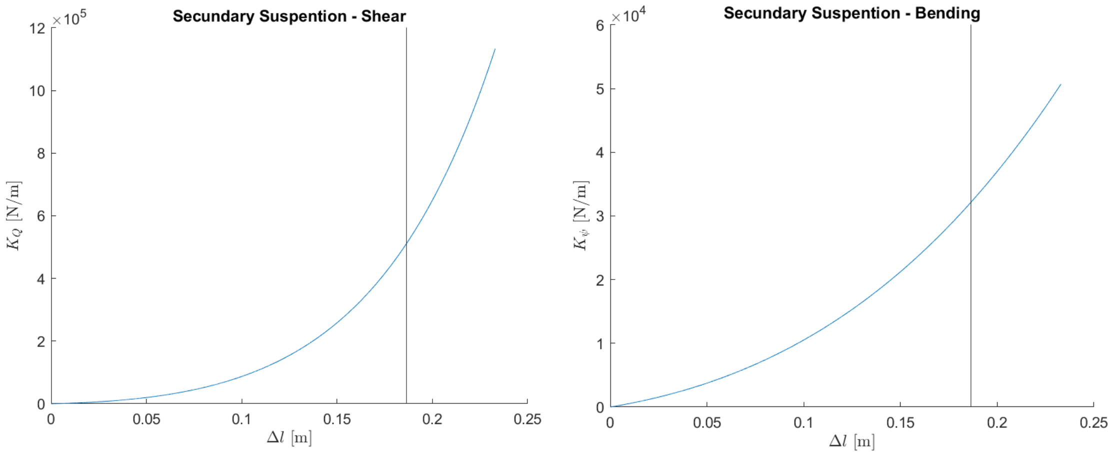

(a) (b)

Figure 22 - Variation of the shear (a) and bending (b) stiffness depending on the spring elongation, for the secondary springs, with the working axial elongation (vertical black line).

The stiffness value selected as an approximation was determined by the working axial load expressed by the manufacturer as 73.5 kN, corresponding to 186.3 mm compression. The values determined can be seen in Table 12.

Table 12 - Stiffness data for the secondary suspension springs, being K_z the axial stiffness, K_Q shear stiffness and K_ψ the bending stiffness

$\boldsymbol{K_z}$	$\boldsymbol{3.94 \cdot 10^5}$ **N/m**
$\boldsymbol{K_Q}$	$5.11 \cdot 10^5$ N/m
$\boldsymbol{K_\psi}$	$3.21 \cdot 10^4$ N/m

In the secondary suspension, damping is achieved by 3 types of dampers: vertical, transverse, and anti-yaw. The first two were modeled similarly by a spring and damper in series, with both damping and stiffness defined as constants. In Table 13, the values defined for these dampers can be seen. Since there was a lack of information, these were defined taking into account examples in the literature [56, 71-74] and manufacturers information. This was also the reason for the implementation of linear models for the damping and stiffness.

Table 13 - Stiffness and damping properties of the transverse and vertical dampers

Damper	Damping	Stiffness
Transverse	35 kNm/s	5 MN/m
Vertical	35 kNm/s	5 MN/m

Although, in the case of the anti-yaw damper the lack of information regarding the current equipment in ARCO, in this case a linear damping would not correctly represent the behaviour of this damper. Once again, a spring and a damper in series model, and literature examples and manufacturers data were used [71, 72]. The considered stiffness was $K = 3.75 \cdot 10^3$ kN/m, the damping function can be seen in Figure 23.

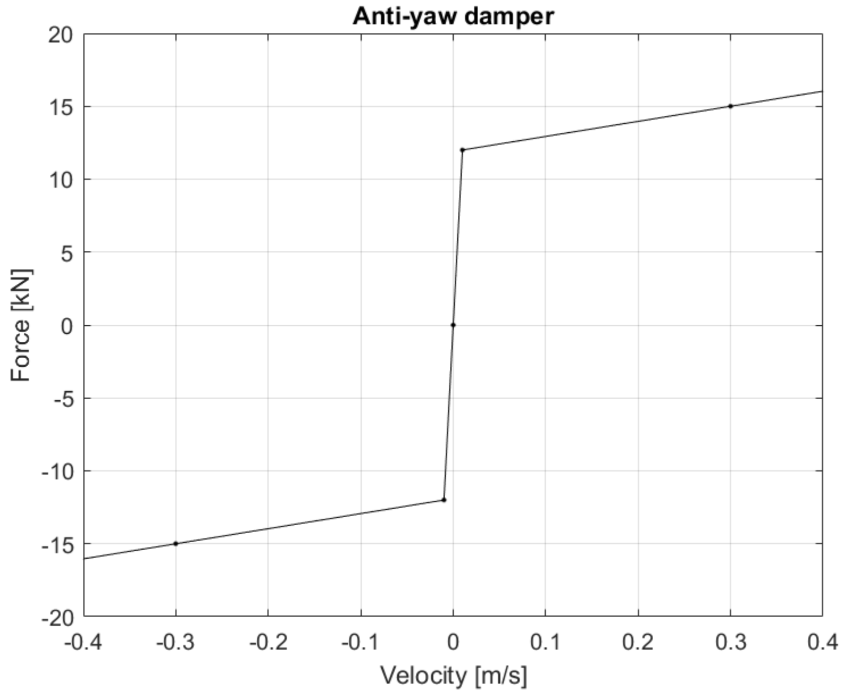

Figure 23 - Damping function of the anti-yaw damper, displayed in force [N] by velocity [m/s].

Besides the spring and damper elements, there are two more relevant structures: the bump stop, the anti-roll bar, and traction rod.

The traction rod (see Figure 20-1) has the purpose of transferring the power from the rail car to the wheels, and in this case consist of a pivot connected to the car body and to two connecting rods, by a flexiblock. These are connected to the bogie structure with an axial hinge. The traction rod was simulated as a cylindrical spring. According to the manufacturer [66] documentation the axial stiffness is 3.38 MN/m and the radial stiffness equal to 95 MN/m, which means an almost rigid connection.

The bump stop (Figure 20-4) is defined in two directions. The bump stops limit the traction rod movement in both x and y directions, in 15 mm and 35 mm, respectively. In Figure 24 the functions used to define the bump stops stiffness in both directions are shown, with these functions corresponding to the relation between force [N] and displacement [m], defined based on the literature [75].

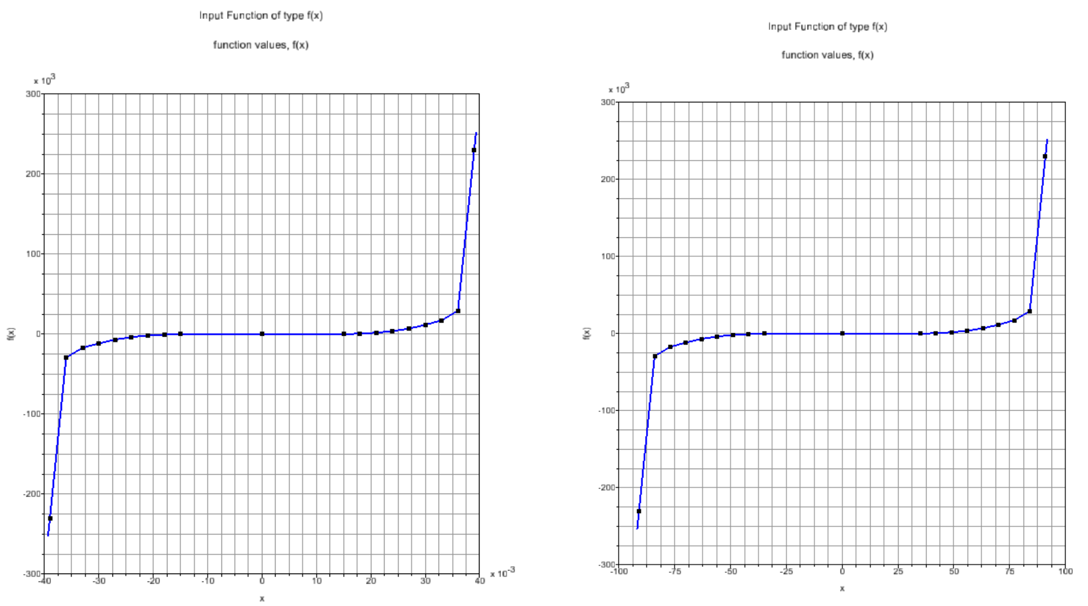

(a) (b)

Figure 24 - Bump stop functions in x (a) and y (b) directions, used to define the nonlinear stiffness [75].

Finally, the anti-roll bar is design to reduce the car body role movement. As seen in Figure 20-3 two pairs of connecting rods are connected to a torsion bar (not in the figure), rigidly, the material tortional stiffness will be the mechanism that will prevent the roll movement.

It was simulated as a rotational spring with stiffness, K_{α}. To define this stiffness, it is considered half of the system and following formulae, where (4.1) defines the bar stiffness [55], the remaining are obtained from the geometry of the mechanism:

$$k_{bar} = \frac{G \cdot I_{yy}}{Y} \tag{4.1}$$

$$T_{\alpha} = Y \cdot F_z = \frac{Y}{X} \cdot T_{\beta} \tag{4.2}$$

$$\beta(t) = \frac{z(t)}{X} \tag{4.3}$$

$$z(t) = \frac{Y}{2} \cdot \sin \mathrm{\alpha(t)} \approx \frac{Y}{2} \cdot \mathrm{\alpha(t)} \tag{4.4}$$

$$T_{\beta} = k_{bar} \cdot \beta(t) \Leftrightarrow \tag{4.5}$$

$$\Leftrightarrow \frac{X}{Y} \cdot T_{\alpha} = \frac{G \cdot I_{yy}}{Y} \cdot \frac{Y}{2 \cdot X} \cdot \ \mathrm{\alpha(t)} \tag{4.6}$$

$$K_{\alpha} = \frac{T_{\alpha}}{\alpha(t)} = \frac{1}{2} \cdot \ G \cdot I_{yy} \cdot \frac{Y}{X^2} \tag{4.7}$$

where:

- k_{bar} is the bar torsional stiffness;
- G is the material shear modulus;
- I_{yy} is the polar moment of inertia;
- $\beta(t)$ is the torsion bar rotation in the axial direction;
- X is the distance in the x direction between connecting rods connection in the bogie structure and the bolster;
- Y is the length of the torsion bar, equal to the distance between the connecting rods;

- $z(t)$ is the movement in the z direction measured in the connecting rod connection in the bolster;
- $\alpha(t)$ is the car body rotation in the x direction, measured in the middle of the bolster dummy;
- T_α is the torque applied to the car body, due to F_z;
- F_z is the force applied to the bolster dummy, due to the torsion bar in the z direction.

Using the data obtained from the documentation displayed in Table 14 and applying equation (4.7) we obtain the stiffness value k_α, also in Table 14.

Table 14 - Data from ARCO documentation for the calculation of the anti-roll stiffness and the result k_α

$\boldsymbol{X}$	$\boldsymbol{Y}$	$\boldsymbol{I_y}$	$\boldsymbol{G}$	$\boldsymbol{k_\alpha}$
$270\ \mathrm{mm}$	$400\ \mathrm{mm}$	$1.222 \cdot 10^{-5}\ \mathrm{m}^4$	$81.5\ \mathrm{GPa}$	$2.88\ \mathrm{MN} \cdot \mathrm{m/rad}$

4.2.3 Bodies

The Bogies of the Arco passenger cars are formed by 3 different type bodies:

- Main structure, responsible for the connection between the primary and secondary suspensions;
- Axle Guide, responsible for the connection between the wheelset and the main frame;
- Bolster, responsible for connection between the bogie and the car body, which will be considered as massless and its mass is integrated in the car body.

4.2.3.1 Main structure

The determination of the mass properties of the bogie was based on a SolidWorks model done in the Experimental and Computational Project of Henrique Oliveira [76] (see Figure 25). The results for the mass, inertia, and location of the centre of mass can be seen in Table 15 and Table 16 .

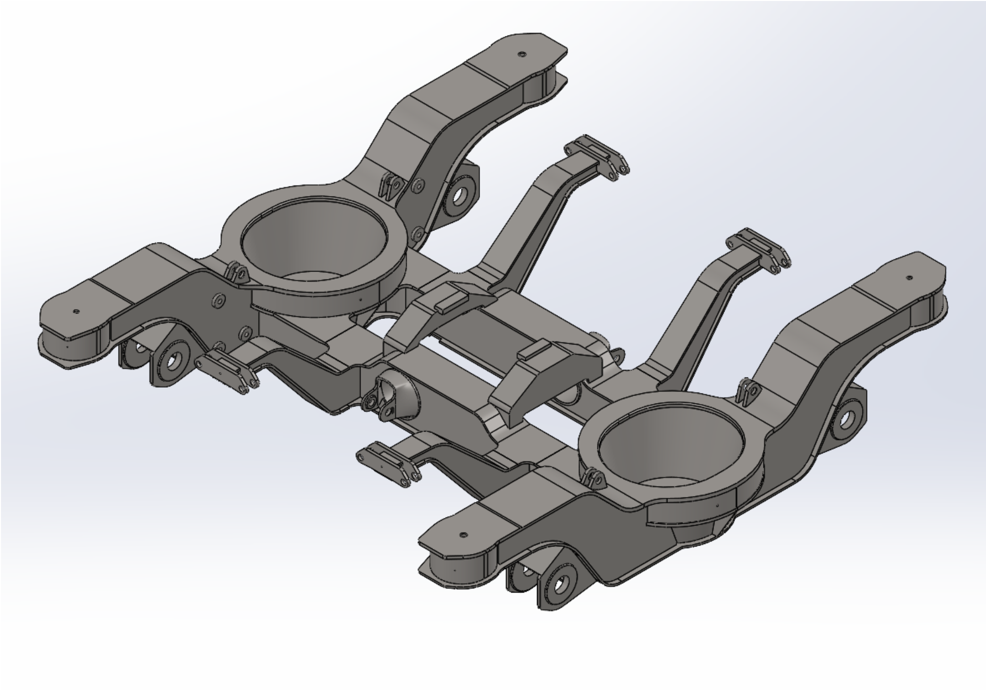

Figure 25 - SolidWorks model of the bogie strcuture developed in [76].

Table 15 – Inertia properies of the bogie main structure, obtained in the centre of mass

Mass	3577 kg
$\boldsymbol{I_{xx}}$	$3200\ \mathrm{kg} \cdot \mathrm{m}^2$
$\boldsymbol{I_{yy}}$	$1313.5\ \mathrm{kg} \cdot \mathrm{m}^2$
$\boldsymbol{I_{zz}}$	$4270.8\ \mathrm{kg} \cdot \mathrm{m}^2$
$\boldsymbol{I_{xy}}$	$-17.48\ \mathrm{kg} \cdot \mathrm{m}^2$
$\boldsymbol{I_{xz}}$	$-0.90\ \mathrm{kg} \cdot \mathrm{m}^2$
$\boldsymbol{I_{yz}}$	$4.06\ \mathrm{kg} \cdot \mathrm{m}^2$

Table 16 - Location of the centre of mass of the main structure, considering the defined coordinate system

Axis	**Location [m]**
$\boldsymbol{x}$	0 m
$\boldsymbol{y}$	0 m
$\boldsymbol{z}$	-0.297 m

4.2.3.2 Axle guide

The axle guide mass properties were determined using a feature of the software SimPack, that calculates them from the geometry definition. This was used, since the Axle guide has a simple geometry (see Figure 17), which could be inputted in the software. The joint of this body was defined as revolving around the wheelset. It was also used a bushing to simulate the joint between the axle guide and the bogie structure.

4.2.3.3 Bolster

To better build a model should be included a bolster body in the bogie sub model. However, this should not have mass or inertia and should be included in the car body properties.

4.3 Wheelset

Although the Wheelset is part of the bogie, its modelling is done separately (see Figure 26), considering that there are two similar wheelsets in each bogie. This model includes the definition of the mass properties of the wheel set, as well as the definition of the rail-wheel contact.

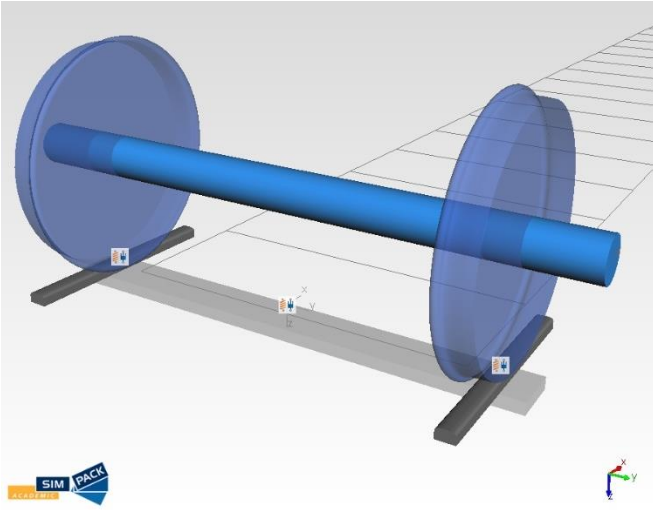

Figure 26 - Wheelset model

The mass properties where introduced manually and are based on the model done by Henrique Oliveira [76]. The result consists of the mass and inertia matrix that can be seen in Table 17. The centre of mass coincides with the origin the body reference marker. This is predefined in the middle point between the two wheels and in their axis. Since the wheelset is a revolution body and symmetric in the other direction, the location of the CG can be easily explained, as well as $I_{xy} = I_{xz} = I_{yz} = 0$.

Table 17 – Mass and inertia tensor of the wheelset, obtained in the centre of mass

Mass	1430 kg
$\boldsymbol{I_{xx}}$	$782.48\ \mathrm{kg \cdot m^2}$
$\boldsymbol{I_{yy}}$	$109.27\ \mathrm{kg \cdot m^2}$
$\boldsymbol{I_{zz}}$	$782.48\ \mathrm{kg \cdot m^2}$

As this rail car was built to operate in the Spanish Iberian gauge lines, the lateral wheel distance is equal to 1729 mm, the wheel radius is equal to 920 mm and the wheel profile is the S1002 (seen in Figure 27).

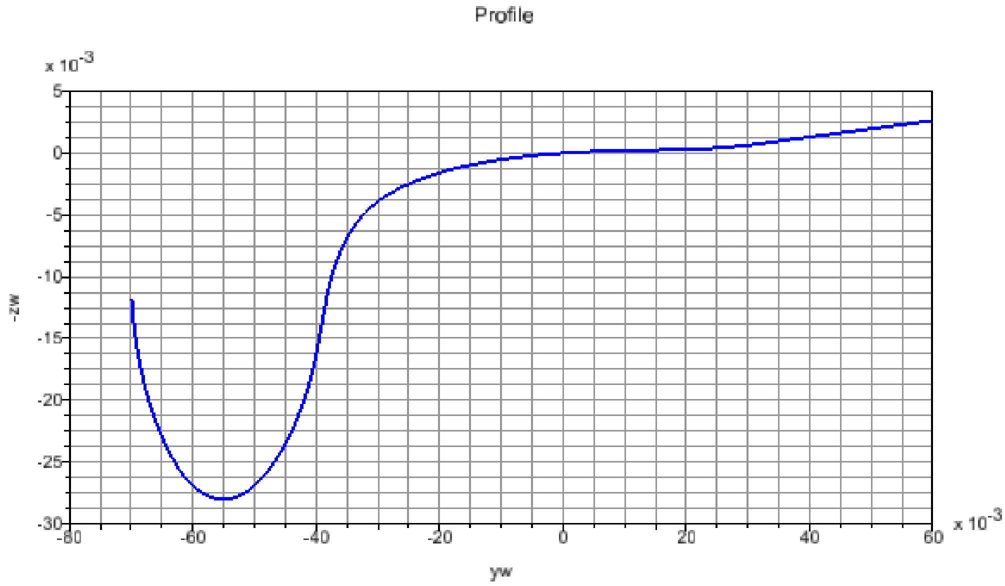

Figure 27 - Wheel profile S1002, defined in SimPack.

4.3.1 Rail-wheel contact

One of the key parameters in Multi-body dynamics in railway is the definition of the Rail-wheel contact. In this case, Hertzian contact was considered with a contact search parameter of 0.0005 meters and a normal damping of 100 kNs/m. Regarding the modelling of tangential contact, the FASTSIM model ("A Fast Algorithm for the Simplified Nonlinear Theory of Contact") was employed for the calculations. The considered friction coefficient was 0.4 and the stick damping and stiffness were respectively 100 MN/m and 1000 Ns/m, respectively.

4.4 Car body

The car body is only defined by mass properties. To determine these, rough estimate was used by building a model in SolidWorks. It was divided into 3 parts: structure; seats; and unspecified structure meant to represent other structures necessary in the operation of the wagon, such as, bathrooms, water tanks or hydraulic system. In [66], the total mass of the car body is 28 t, when empty; and 36 t, when full of passengers.

To define the car body structure geometry, were used the dimensions and geometry defined in Figure 16, retrieved using AutoCAD and applied in SolidWorks were used.

(a) (b)

Figure 28 - SolidWorks model - Car body structure cross section sketch (a) and model (b).

The other types of structures were defined by simple cuboids, in terms of geometry and defined their mass. These were obtained from similar passenger trains [73] and considering the total car body mass, referred previously. In Table 18 the mass associated to each type of part in the car body is shown.

Table 18 - Mass of the components of the car body

Component	Mass
Structure	17926 kg
Seats	1580 kg
Others	11000 kg
Total	35579 kg

The results for the mass and Moments of Inertia of the car body are displayed in Table 19.

Table 19 - Mass properties of the ARCO car body

Mass	**35578 kg**
$\boldsymbol{I_{xx}}$	$43510\ \mathrm{kg} \cdot \mathrm{m}^2$
$\boldsymbol{I_{yy}}$	$1985732\ \mathrm{kg} \cdot \mathrm{m}^2$
$\boldsymbol{I_{zz}}$	$1989457\ \mathrm{kg} \cdot \mathrm{m}^2$

It is also relevant to the multi-body dynamic simulation to compute the location of the centre of gravity. These results can be seen in Table 20, the reference system is located in the middle of the track at mid-point between the two bogies.

Table 20 - Location of the centre of gravity

Axis	CG Location
$\boldsymbol{x}$	0
$\boldsymbol{y}$	0
$\boldsymbol{z}$	-1.0 m

4.5 Simpack model

The modelling of the wagon was built in three parts, the wheelset, the bogie, and the car body.

In Figure 29, he final model in SimPack can be seen, and it is important to note that the global coordinate system is defined as $x\ axis$ in the track direction, $y\ axis$ in the lateral direction and $z\ axis$ in the vertical direction, pointed downwards.

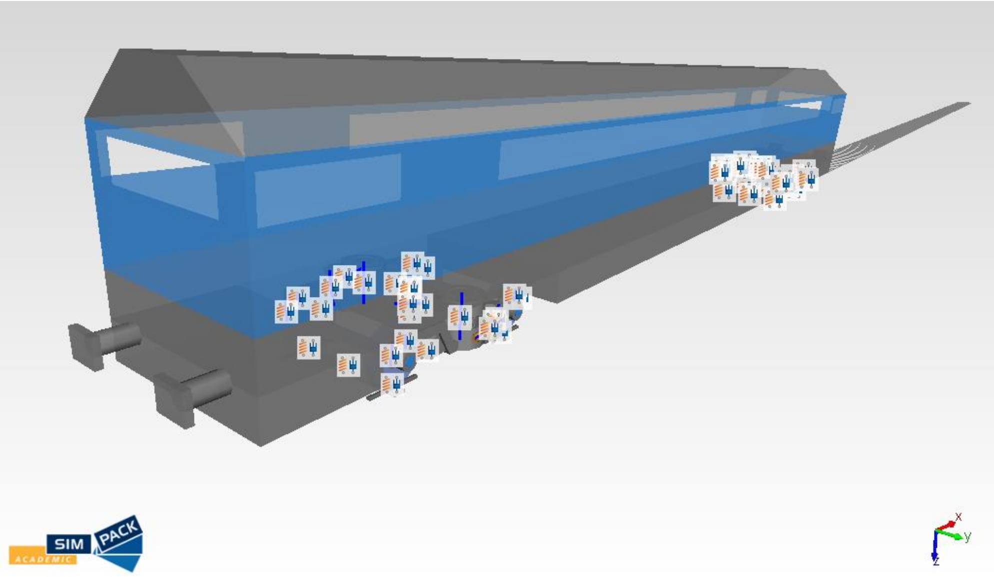

Figure 29 - Final global SimPack model

SimPack modellling is done using several types of elements, to perform the multi-body simulation. The system mass is given by bodies, the stiffness and damping are determined by force elements. Several other definition and analysis results can be added to the model, in order to easily change between simulation configurations. The degrees of freedom (DoF) are defined using joints (one of the possibilities of defining the constraints in SimPack), each body has only one joint associated, and these act as boundary, restriction to the system of equations. To define the mass properties, the points of the location of force elements and the point where joints are applied are used markers, which are fixed or moving connection points, with local coordinate systems. These can be associated to a body or to a reference system. Nevertheless, each of those have at least one marker associated to it. The model has a total of 62 DoF.

4.5.1 Bogie

In SimPack modelling, the model is constituted by 2 types of elements: force elements and bodies. The first responsible for the damping and stiffness and the second defines the mass properties of the model. The built bogie model can be seen in Figure 30. The connection between the bogie and the car body is made by a 0 degrees of freedom joint between the bolster and the car body.

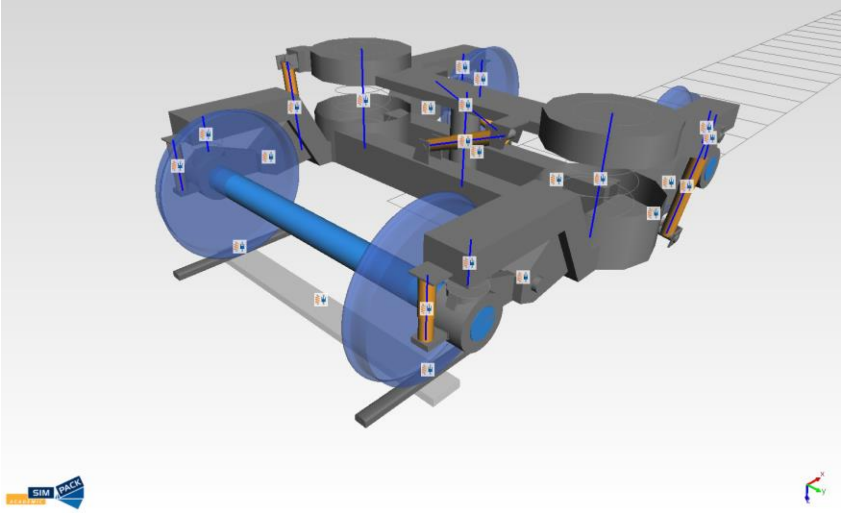

Figure 30 - Simpack model of the bogie.

4.6 Summary of the Chapter

Summarizing, the ARCO passenger cars were a Spanish rail car developed for Renfe and later improved. Recently CP acquired them to add to their fleet of intercity rolling stock. The most complex part of the modelling is the bogie composed by primary and secondary suspensions. The primary suspension consists of springs connecting the axe box and the bogie structure, modelled as shear springs; and damper modelled by a stiffness element in series with a damping element defined by a nonlinear function. The secondary suspension consists of 2 springs, modelled as shear springs; 2 vertical and 2 transverse dampers, modelled as a stiffness element in series with a damping element, both with linear laws; 2 anti-yaw dampers, modelled by a stiffness element in series with a damping element defined by a nonlinear function; a traction rod defined by a spring element with torsional stiffness; a traction rod modelled as a cylindrical spring element; and a bump stop with a non-linear stiffness function.

The car body properties, as well as the wheelset and bogie structure mass properties were estimated using SolidWorks. A standard rail-wheel contact was selected for the model. For the simulation similar settings were used changing only the speed and the track considering the following analysis: Critical speed; Twist test; Dynamic behaviour; Comfort analysis; and behaviour in a track with poor condition.

The following chapter will describe and analyse the results obtained from these simulations.

5 Analysis definition and Results

This chapter shows the definition of the analysis preformed in order to understand dynamic behaviour of the model. Following this definition, the results of the simulations are shown and analysed.

5.1 Analysis

Once the model is defined, it should also be defined the track layout, as well as time integration settings. The chosen integrator was SODASRT2, a backward differentiation formula, an implicit multistep integration scheme besed on the DAST integrator [77]. Regarding the time integration configuration, a sampling rate of 200 Hz, a maximum step size of 0.01 s and a tolerance value of $1 \cdot 10^{-5}$ in absolute terms and $1 \cdot 10^{-10}$ in relative terms were defined.

5.1.1 Critical speed

The critical speed determination is done in a straight track, with sufficient length. This track has a small lateral defect, as shown in Figure 31, composed by a sine curve of half period length, with frequency of 0.628 m^{-1} and amplitude of 5 mm. The train has an initial speed higher than its maximum speed and it is decelerated until it reaches a small speed, 5 km/h in this case. This analysis will be performed with and without the anti-yaw dampers. The initial velocity is 350 km/h.

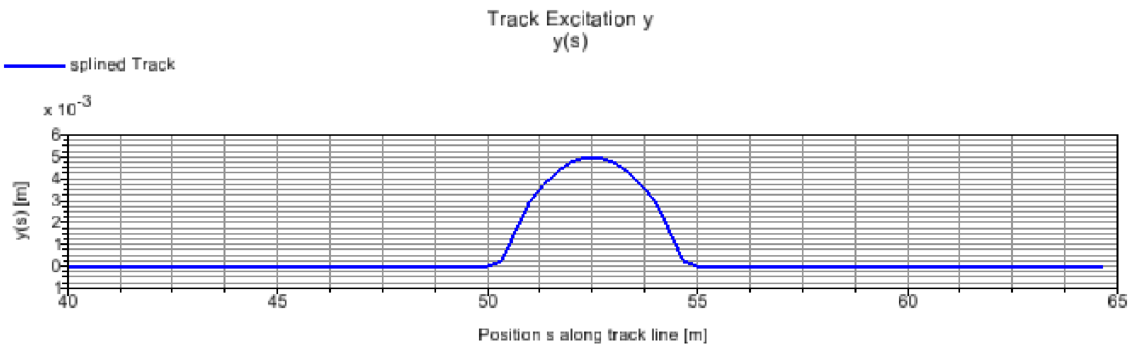

Figure 31 - Defect in the y direction, for the track used for critical speed determination.

5.1.2 Analysis according to EN 14363

As mentioned in subsection 2.6.2, EN 14363 sets several tests to define the railcar dynamic behaviour. In this case both tests were performed.

Considering the twist test, the track was design to perform the test of a vehicle with bogies. The track layout can be seen in Figure 32, showing both the top view and the track curvature, the curve radius is equal to 150 m.

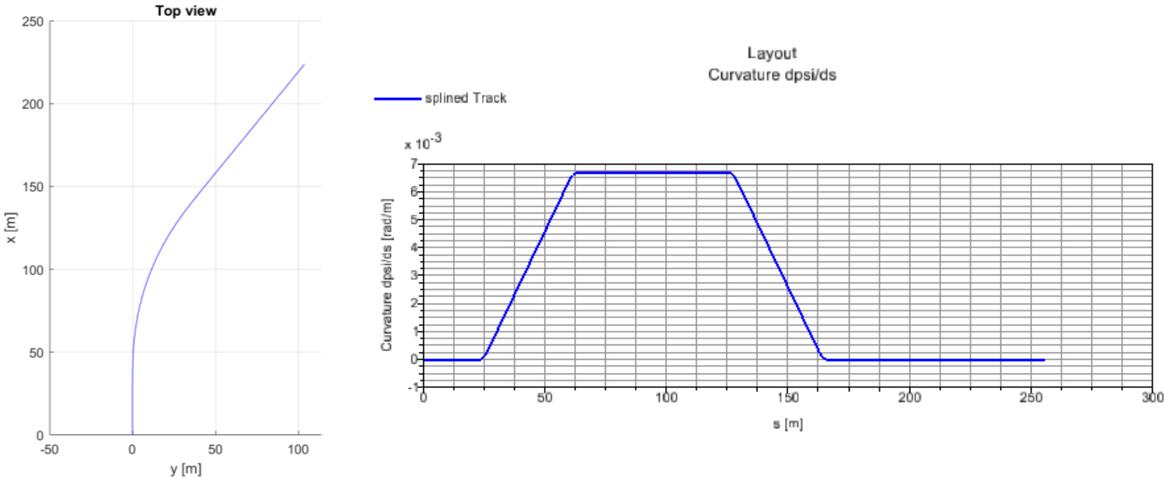

(a) (b)

Figure 32 - Track layout for simulation of the twist test defined in EN 14363 - top view (a) and curvature (b)

As defined in EN 14363, considering the following:

$$2a^* = 18.4 \text{ m} \tag{5.1}$$

$$g^*_{lim} = 3 \text{ ‰} \tag{5.2}$$

$$2a^+ = 2.5 \text{ m} \tag{5.3}$$

$$g^+_{lim} = 7 \text{ ‰} \tag{5.4}$$

The track will assess both bogie twist and car body twist, with a 90 mm cant being utilized to measure car body twist, as depicted in Figure 33, and a dedicated fixture used to examine the bogie twist test, as shown in Figure 34.

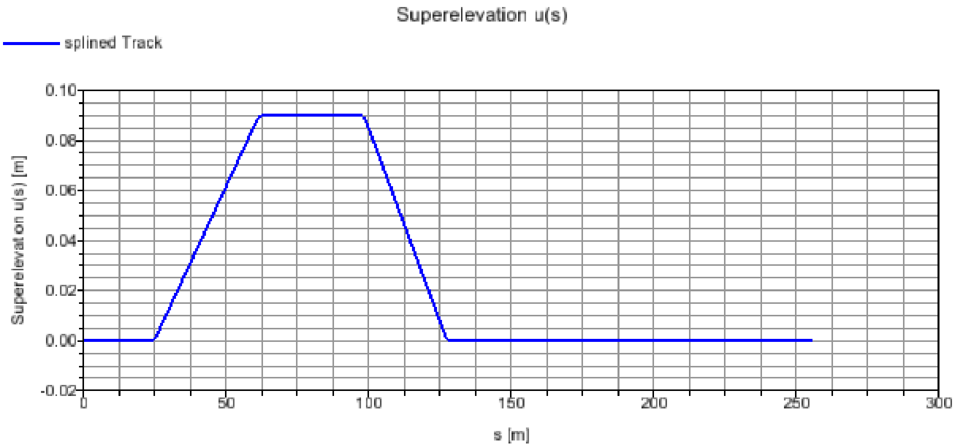

Figure 33 - Superelevation (cant defect) to perform the car body twist test according to EN 14363.

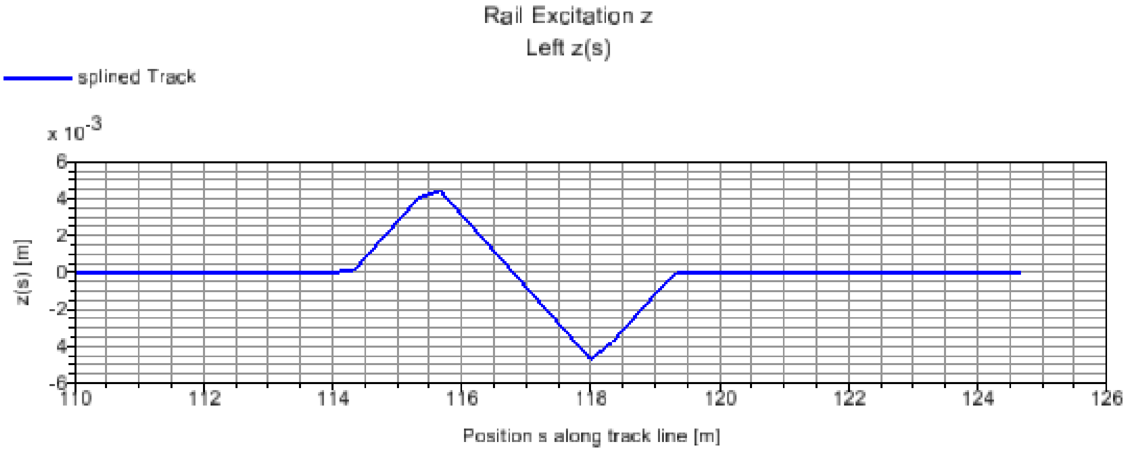

Figure 34 - Track defect design to perform the bogie twist test.

To implement the EN 14363 procedure, a track was structured into four sections, mirroring those outlined in the standard. These sections comprise five different curve radii (as depicted by the curvature in Figure 36-a , varying cant (as evident in the superelevation in Figure 36-b) and differing lengths. The testing speed was defined as $V = 1.1 \cdot V_{adm} = 1.1 \cdot 200 = 220\ \mathrm{km/h}$.

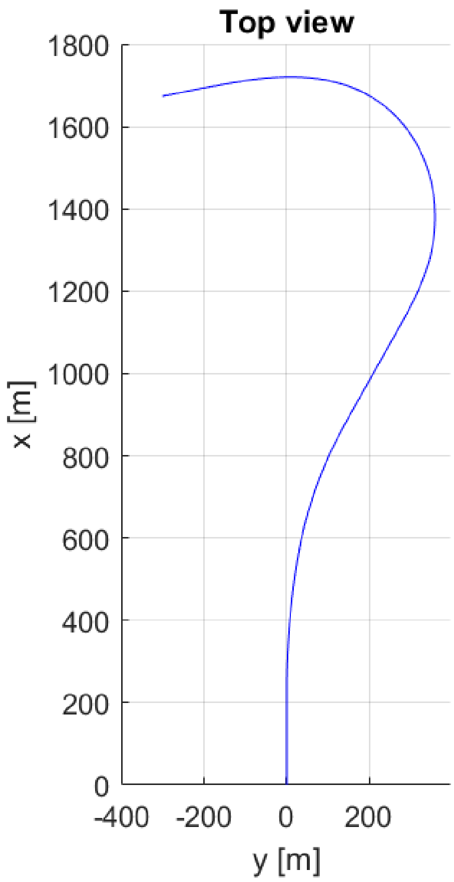

Figure 35 - Track layout top view designed according to EN 14363.

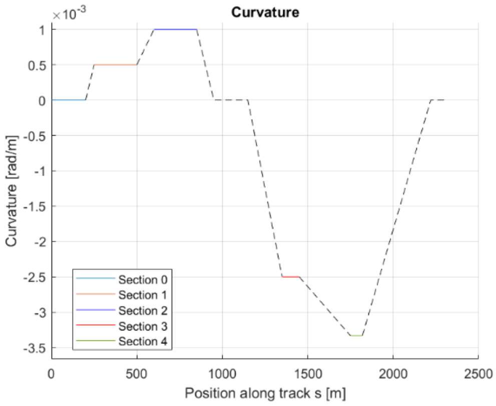

(a)

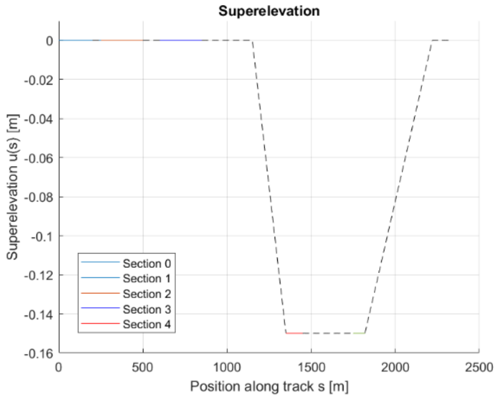

(b)

Figure 36 - Track definition, according to EN 14363 for dynamic testing, showing curvature (a) and superelevation (b) along the track length.

Throughout the two test and to better mimic the reality, speed was not introduced directly to the rail car, it was added a mass connected to the coach by a spring, which acted as a locomotive.

5.1.3 Behaviour in track with poor conditions

To obtain the behaviour of the model in real conditions a model of a track section where an accident occurred was used. On the 1st of April 2017, a train derailed when arriving to Coimbra, in *Linha do Norte*¸ it was concluded that the accident occurred due to bad infrastructure conditions. However, not all wagons derailed, the locomotive, which had secondary suspension did not derail. The *Gabinete de prevenção e investigação de acidentes com aeronaves e acidentes ferroviários (GPIAAF)* resorted to FEUP to develop a multi-body dynamics model to simulate the incident. During that work, the defects on the track were determined and applied in this thesis. The track section consists of a straight followed by one left and one right curve as shown in Figure 37. The track was in poor conditions and was undergone by maintenance that led to worst condition. This means that the track was severely defected as shown in Figure 38 and Figure 39. Concerning speed, a similar approach was applied as per the analysis outlined in EN 14363 (see subsection 2.6.2), and the testing encompassed a range of speeds between 80 km/h and 150 km/h. The actual accident occurred at 90 km/h, but occurred in freight wagons [78, 79].

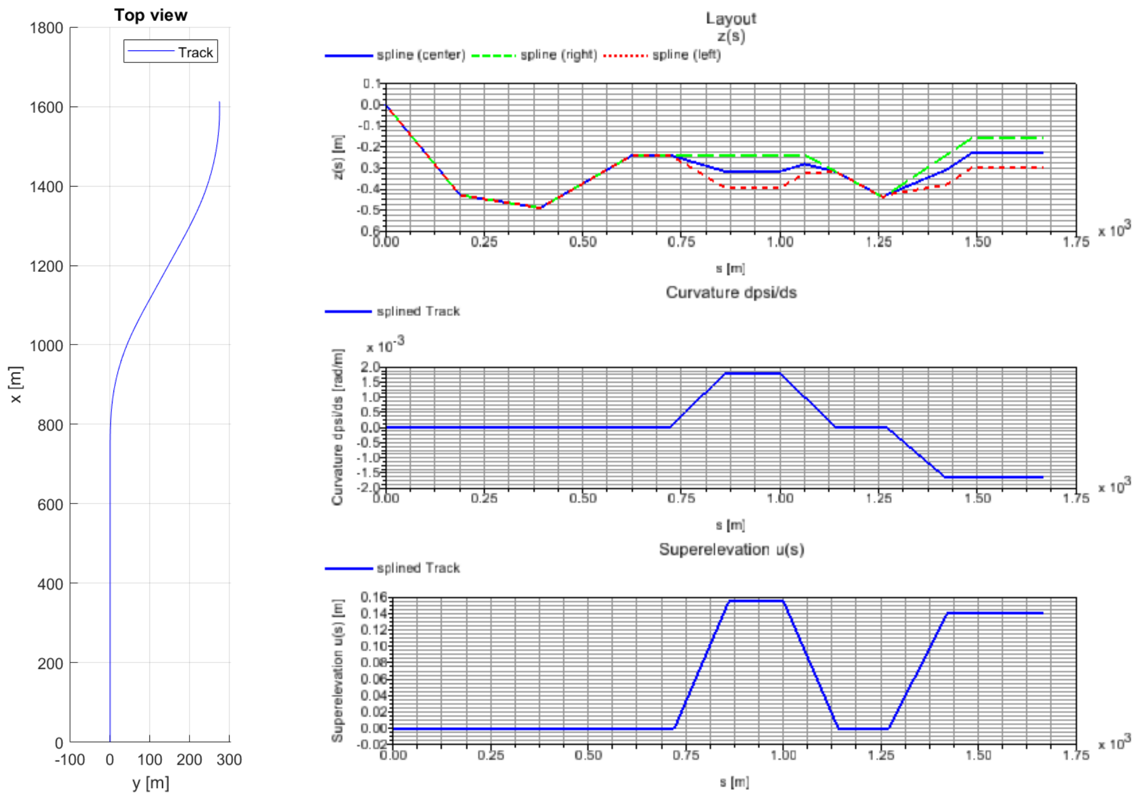

(a) (b)

Figure 37 - Track layout in x-y (a) and x-z directions (b), curvature (b) and superelevation (b) for the accident track section in *Linha do Norte*.

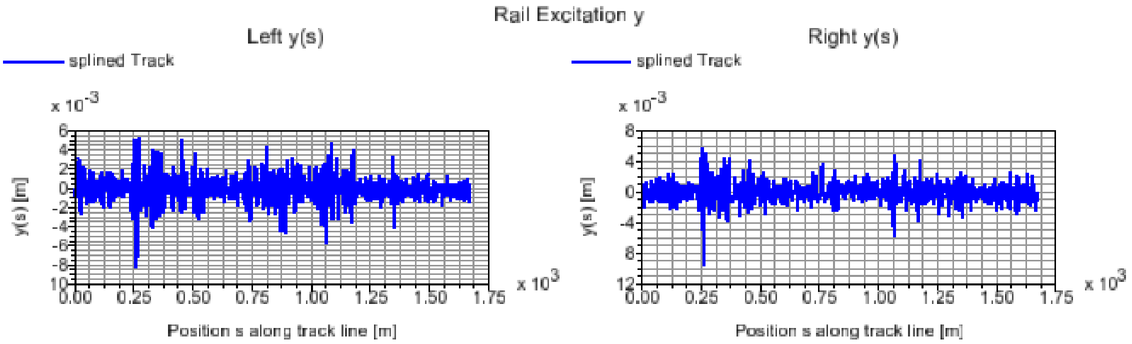

Figure 38 - Track defects in the y [m] direction along the track [m] for the accident track section in *Linha do Norte*.

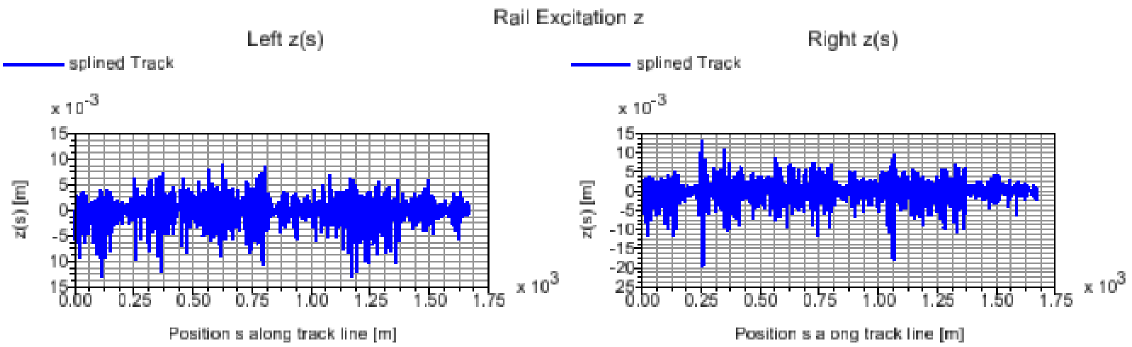

Figure 39 - Track defects in the z [m] direction along the track [m] for the accident track section in *Linha do Norte*.

5.1.4 Comfort analysis

In order to evaluate the ride comfort of a rail car is necessary to test it in a defected track. To evaluate the response to the defect a straight track was used. The excitation of the track defined in SimPack was obtained from available databases [77]. In Figure 40 and Figure 41, are shown the first derivatives, to be noticeable the minor irregularities within the broader shape.

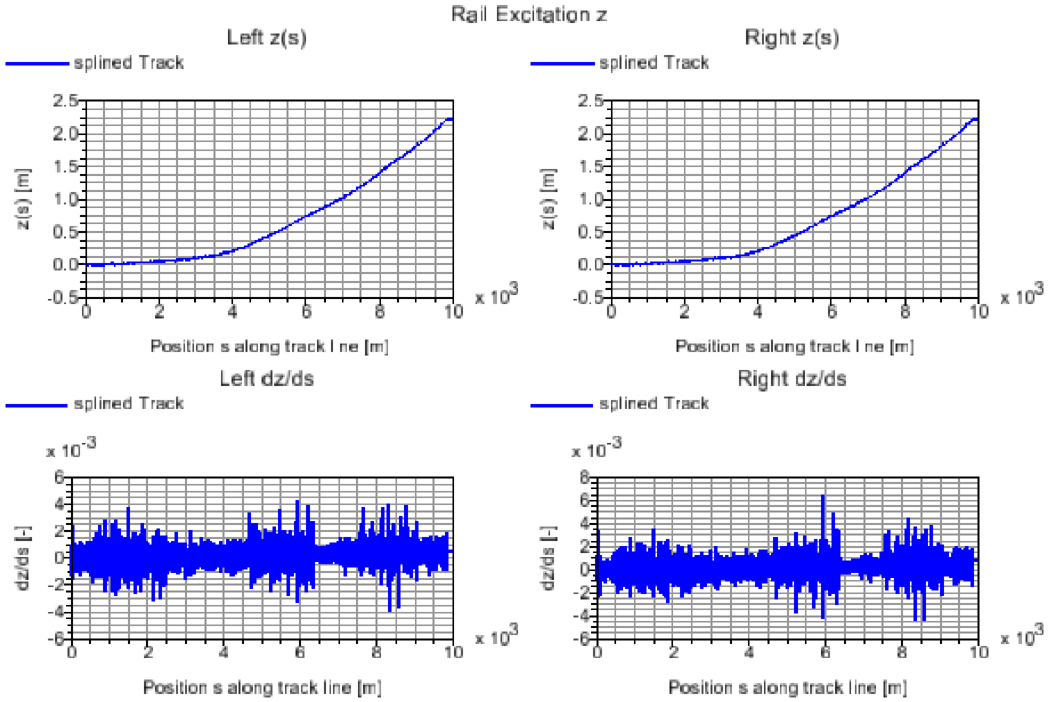

Figure 40 - Track defects in the z direction used for evaluating the ride comfort.

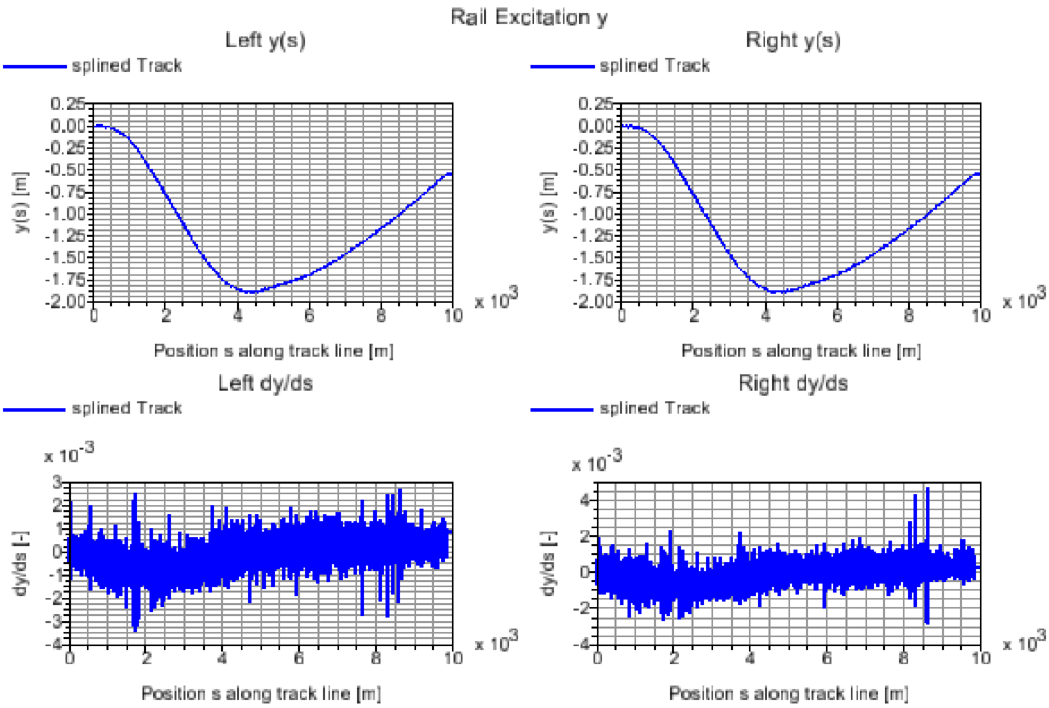

Figure 41 - Track defects in the y direction used for evaluating the ride comfort[77].

5.2 Critical speed

As mentioned in Section 4.1, the maximum operation speed established for this vehicle is 200 km/h, after the addition of the anti-yaw dampers. The determination of the critical speed should be done at a speed higher than the train maximum speed, so the testing speed was 350 km/h. It was predictable a critical speed slightly higher than the maximum speed.

However, at this speed there was no hunting movement instability. The simulation was run again with a velocity of 650 km/h.

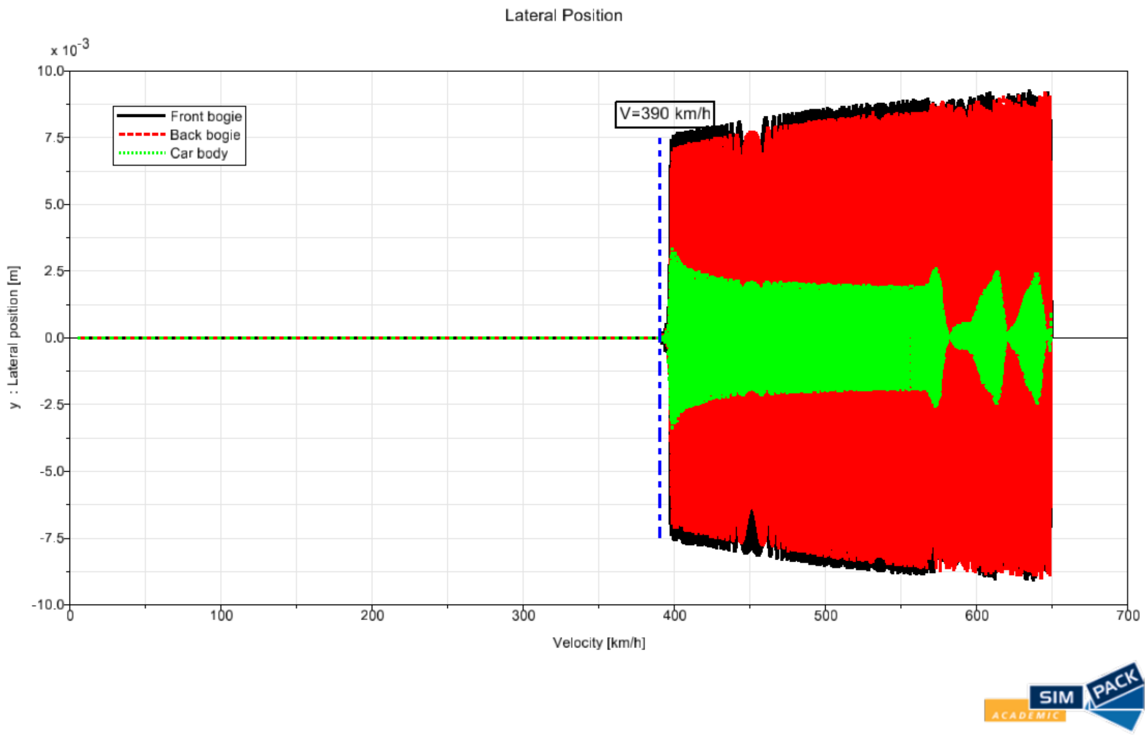

Figure 42 - Results of the non-linear critical speed analysis, with an initial velocity of 650 km/h, showing the lateral displacement of the car body and both bogie main structures.

The results of this analysis can be seen in Figure 42, the graph was made corresponding each point in time to its speed, since there is a linear deceleration, each speed only occurs once. In this figure the critical speed is equal to 390 km/h, which is almost double the railcar maximum speed. It is relevant to mention the fact that the car body instability movement is not constant, as one can see points of reduction of this instability.

In its first version, the ARCO passenger car had as its maximum speed 160 km/h, without yaw dampers. For this reason, the same simulation was done without these dampers. In this case the initial speed was again 350 km/h. In Figure 43, the results of this analysis can be seen. In this case can be seen a reduction of the instability around 127 km/h, although, a more consistence reduction can be seen around 105 km/h. The car body movement is more unstable without the yaw dampers, displaying a higher movement amplitude. Furthermore, a less abrupt reduction in the hunting movement around the critical speed can be seen. This may be explained due to the undamped movement when the train operates at that speed.

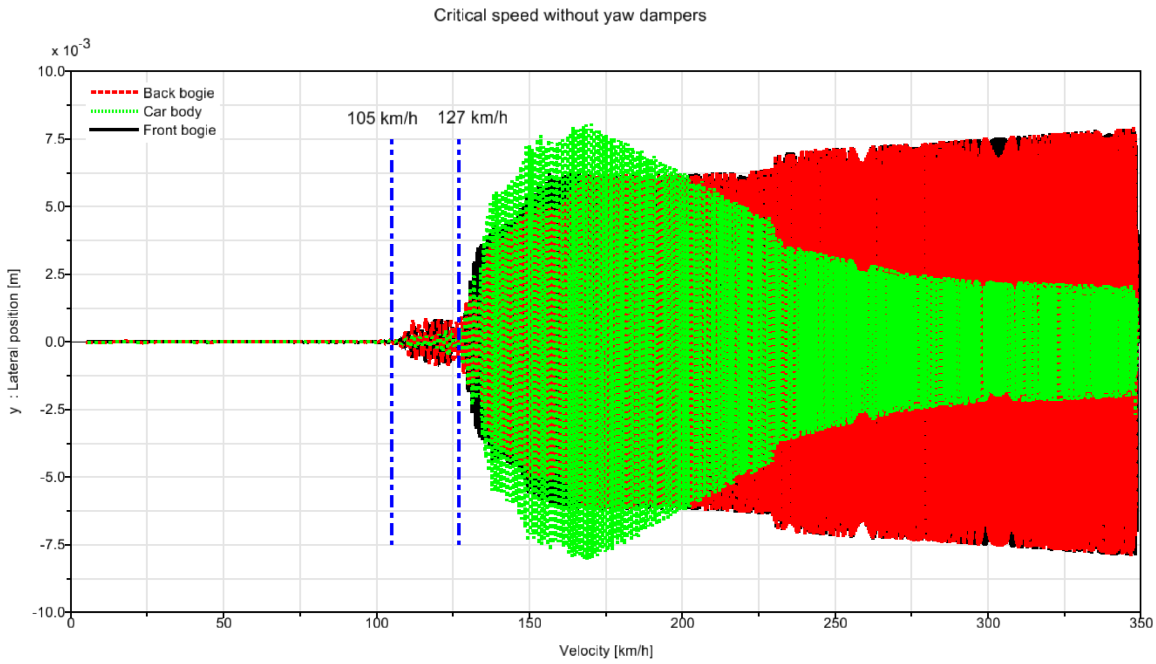

Figure 43 - Results of the non-linear critical speed analysis of the railcar without yaw dampers, with an initial velocity of 350 km/h, showing the lateral displacement of the car body and both bogies main structures [m], by the velocity [km/h].

These critical speed results are also bellow the expected one, since the previous version had a maximum speed of 160 km/h. This possibly means the damping or mass modulations do not represent the reality of the rail car. The stiffness and damping of the secondary suspension dampers could influence these results.

The damper stiffness will influence at which frequencies there will be a bigger damping, i. e. at which speeds the damper will have a bigger effect. Regarding the mass definition will lead to different natural frequencies of vibrations which will impact the hunting movement frequency.

5.3 Analysis according to EN 14363 – Twist test

The twist test, defined in EN 14363, analyses two relevant outputs: the wheel lift, and derailment criteria, Y/Q, which should be as follows:

- $\Delta z \leq 5$ mm;
- $Y/Q \leq 1.2$.

In Figure 44, the results for the wheel lift for the relevant wheels can be seen, which is always lower than the 5 mm limit, being around 1 mm. In Figure 45, the results of Y/Q can be seen, which even though not mandatory to pass this test are well within the 1.2 limit for the twist test.

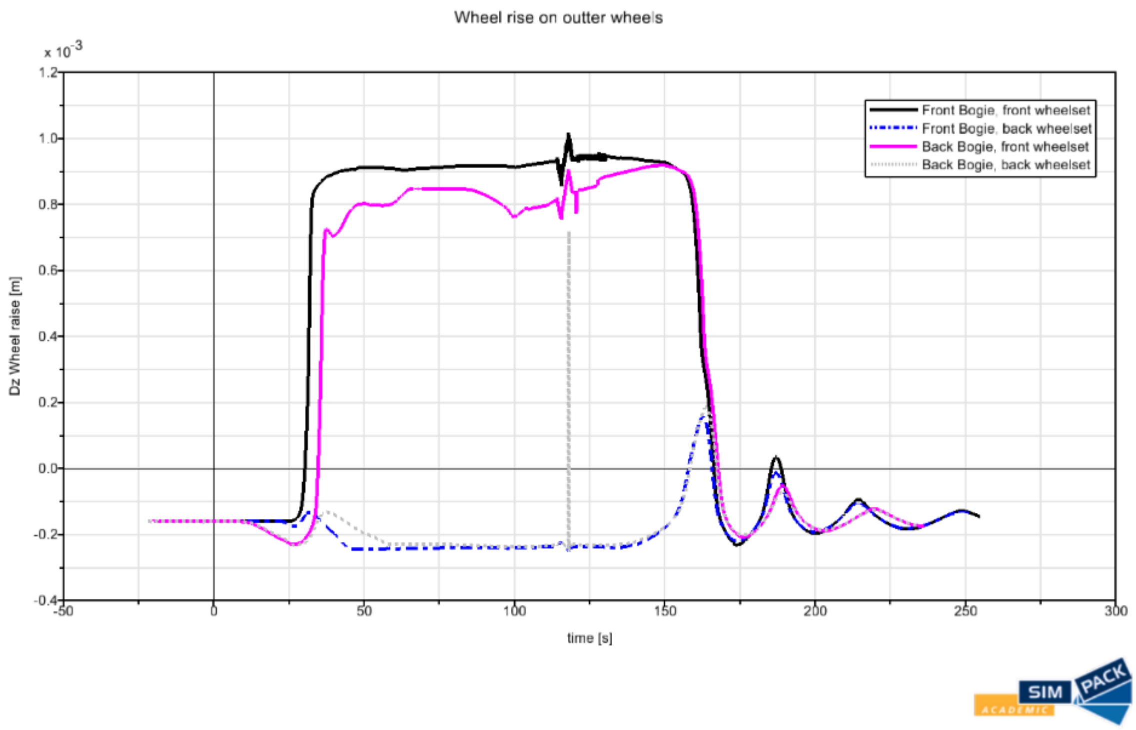

Figure 44 - Wheel raise result for the outer wheels of the wheelsets [m], along the track [m].

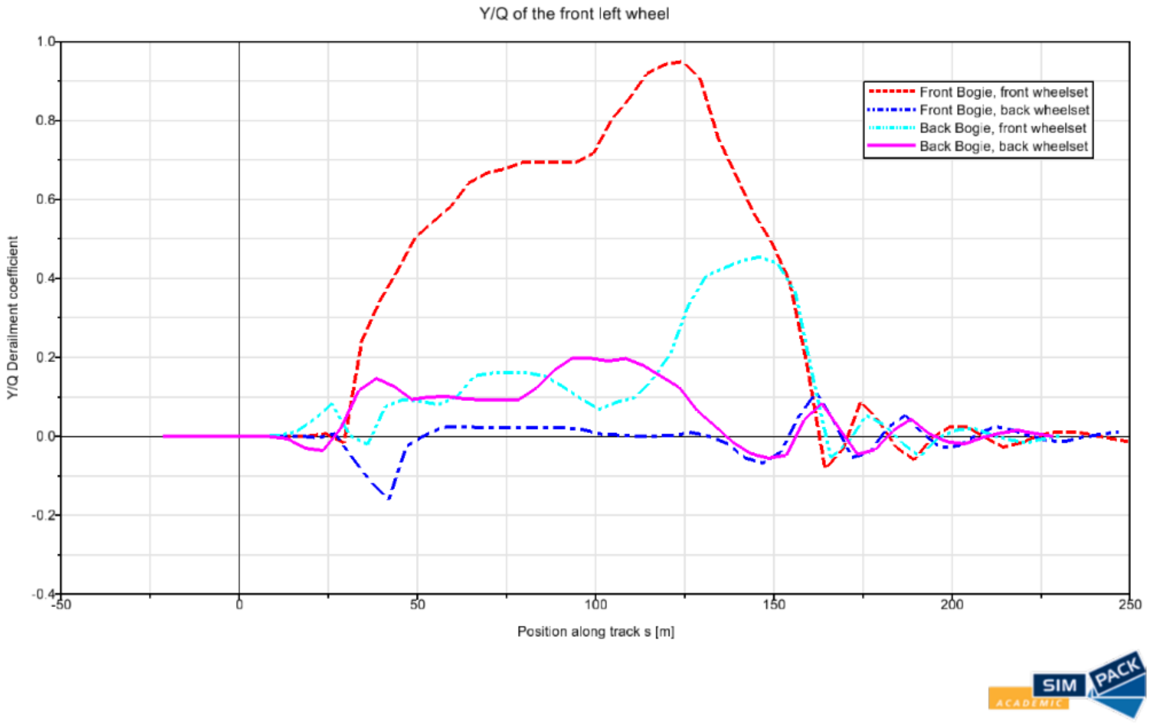

Figure 45 - Results for the Y/Q derailment criteria for the outer wheels of the wheelsets, along the track [m].

5.4 Analysis according to EN 14363 – Dynamic behaviour

This test is aimed at evaluating the global behaviour of the rail car. As mentioned in subsection 2.6.2, this test defines several measures, that should be evaluated. As defined in the standard the test speed used was $1.1 \cdot V_{adm} = 220$ km/h, however, this speed leads to a derailment in section 4 of track. Considering this result, simulations with decreasing speeds were performed, until there was no derailment in this track section.

Since, the curve with the smaller radius is to the left, the analysed wheel will be the front right, the most critical, due to being the front and outer wheel. As the analysis done before shows, this is the most critical wheel-rail interaction.

In Figure 46, one can see, as anticipated, there is a noticeable rise in Y/Q leading up to the derailment at speeds of 220 km/h, 200 km/h, and 180 km/h.

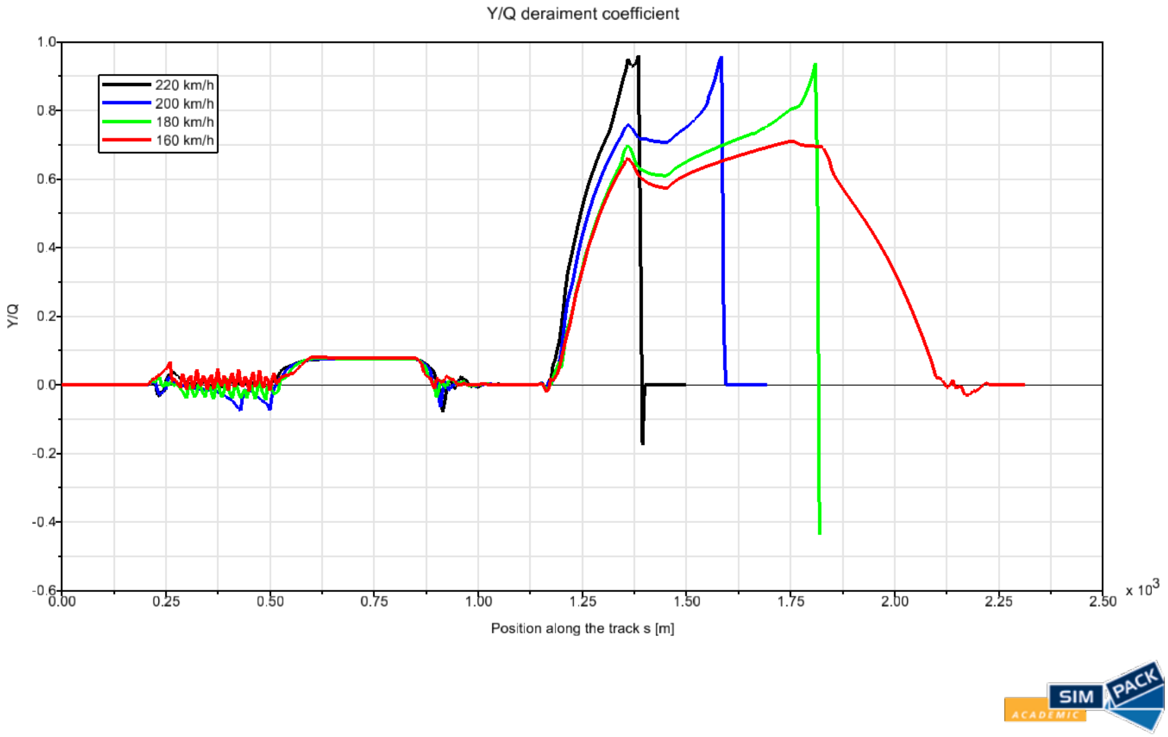

Figure 46 - Y/Q derailment coefficient along the track position [m], for the tested speeds.

The train at 220 km/h derail when arriving to section 3. At 200 km/h, the railcar was not able to keep in track when the radius was smaller than 400 m, at 180 km/h it was still not able to travel in section 4. Only at 160 km/h was the railcar capable of travel the whole track without derailing. This can be confirmed by the value of Y/Q which was always bellow the maximum of 0.8.

Figure 47 shows the sum of the lateral wheel forces f the frontal wheelset.

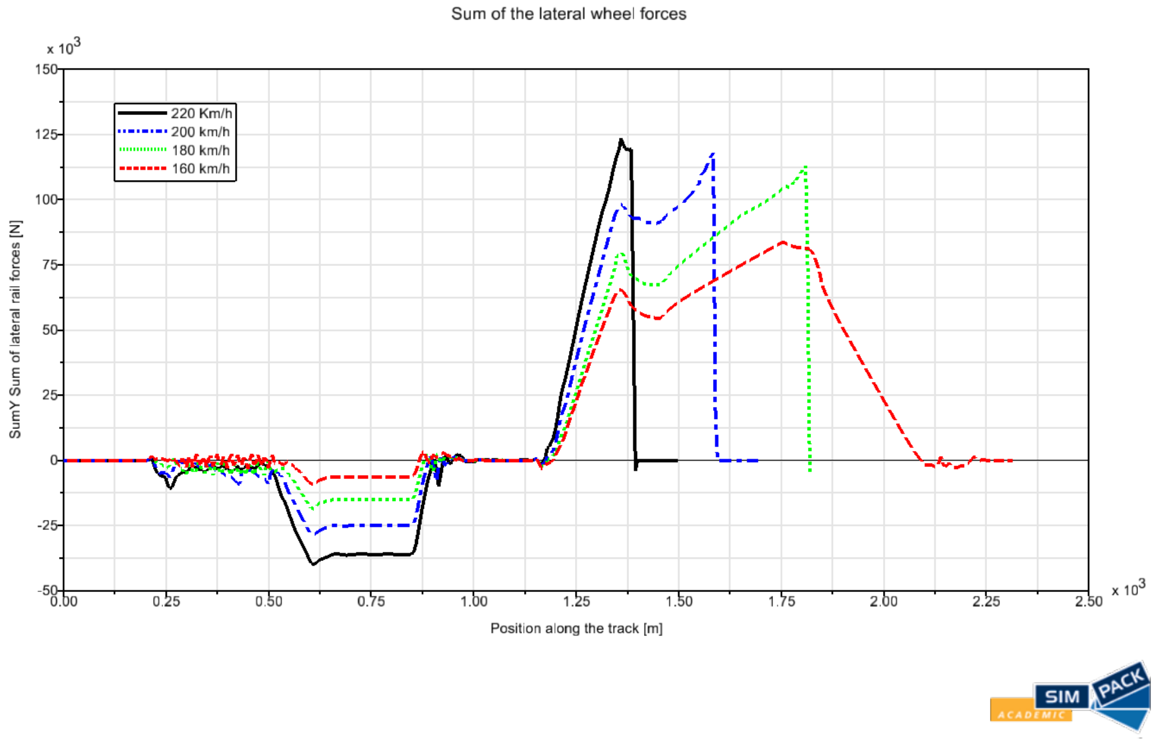

Figure 47 - Sum of the lateral wheel forcers of the frontal wheelset, along the track [m], for the selected speeds.

The standard defines as maximum sum of lateral forces as $k_1(10\,\mathrm{kN} + P_{F0}/3)/2$, which in this case is equal to 19.89 kN, and this limit is set due to the maximum force on the infrastructure. Analysing the graphs, it can be seen that the lateral force exceeds the limit defined in the standard, which means that the maximum speed for this track should be lower.

The lateral acceleration is also limited, also due to passenger comfort, its results can be seen in Figure 48.

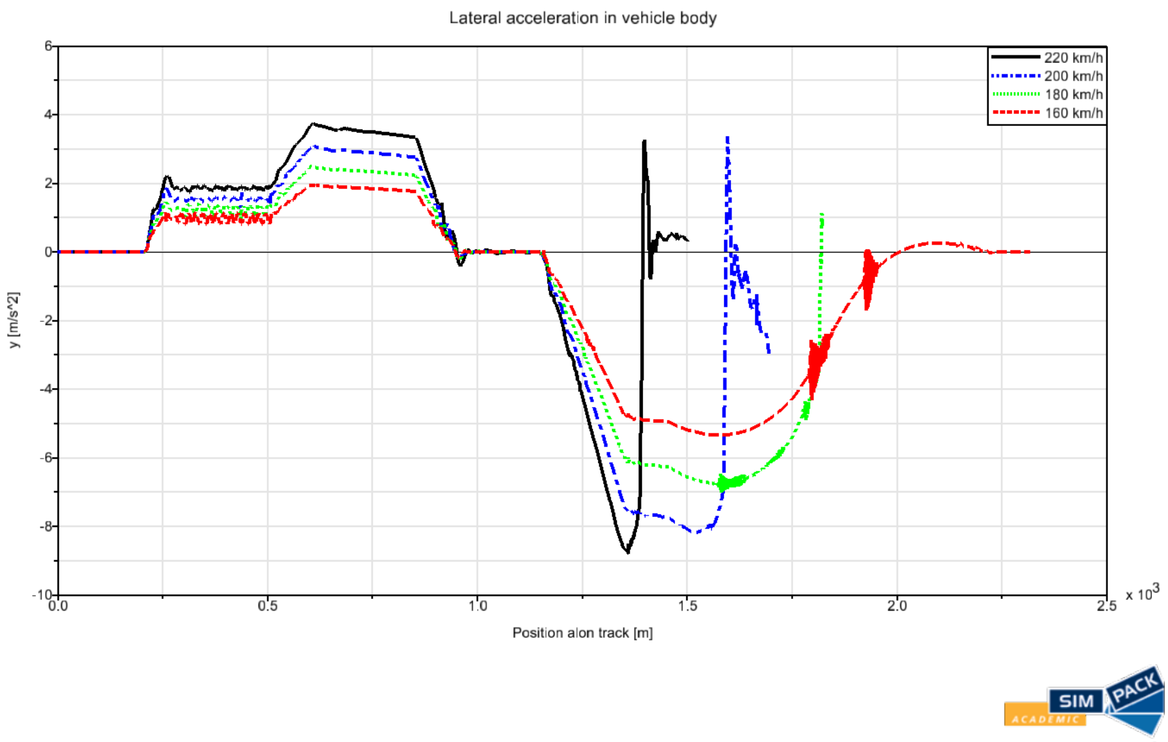

Figure 48 - Lateral acceleration $\ddot{y}^{*}_{m,s}$ $[\mathrm{m/s^2}]$ on the car body along the track, for the defined speeds.

For this parameter, the rail car only complies at 160 km/h, in sections 1 and 2. In all other sections the acceleration value is above the limit of 3 m/s^2. In those sections, the rail car should pass the test at 220 km/h, considering that this is the test speed in those sections. Regarding the vertical acceleration, the results can be seen in Figure 49.

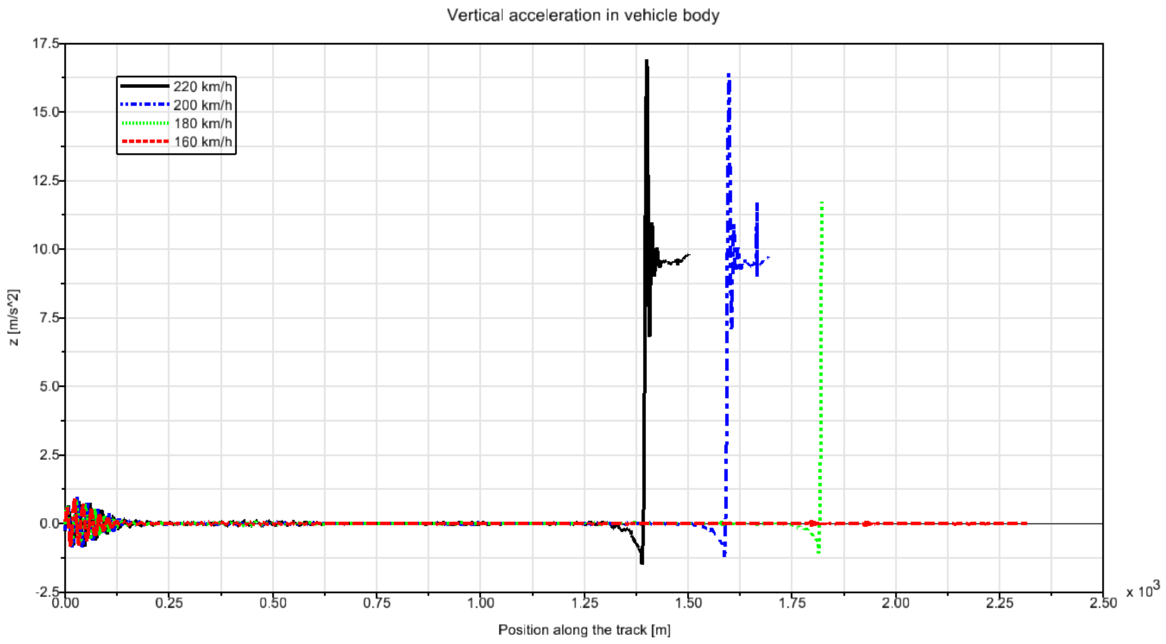

Figure 49- Vertical acceleration $\ddot{z}^*_{m,S}$ [m/s^2] along the track, for the defined speeds.

Contrarily to the lateral acceleration, in this case, the model complies in every speed until the moment of derailment. In the beginning of the simulation can also be seen an increase in vertical acceleration, and this occurs due to initial unbalance of the model.

5.5 Comfort analysis

Regarding the ride comfort analysis, the simulation was done at 200 km/h. The results for the acceleration in the 3 directions, measured in the rail car floor can be seen in Figure 50.

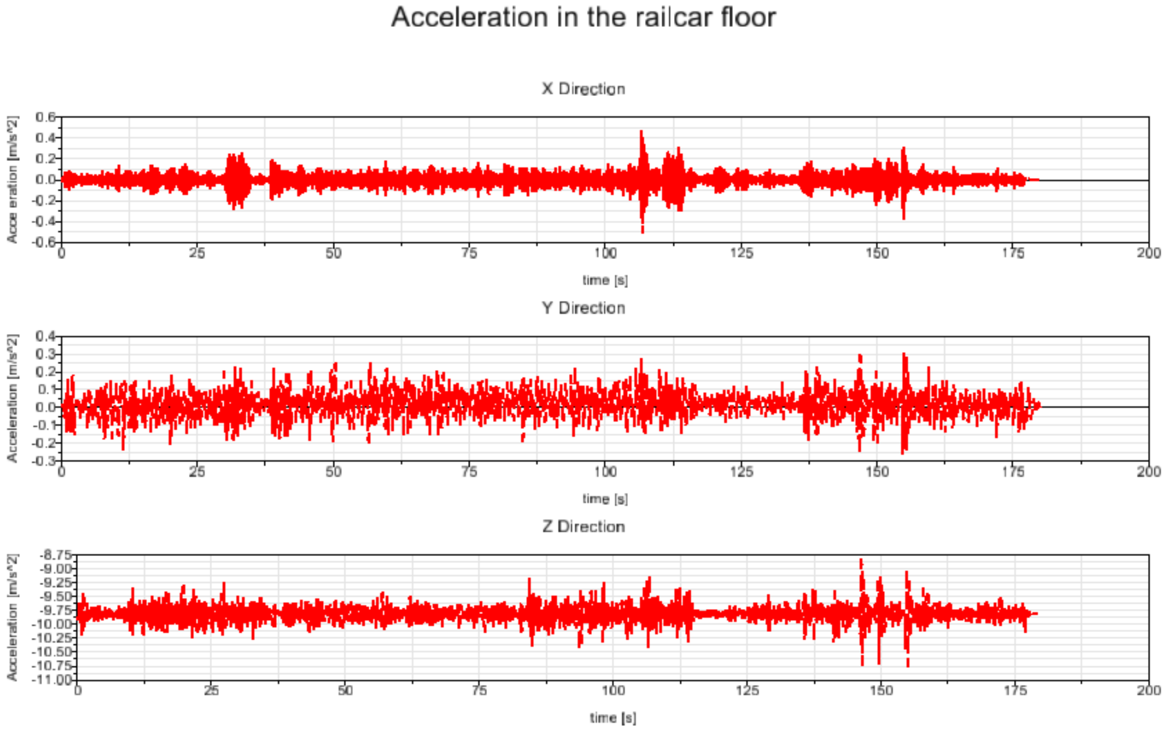

Figure 50 - Acceleration results $[\mathrm{m/s^2}]$ for the comfort analysis simulation, in directions x, y and z, by the simulation time [s].

After applying the filter described in EN 12299 [52], the accelerations are obtained as represented in Figure 51.

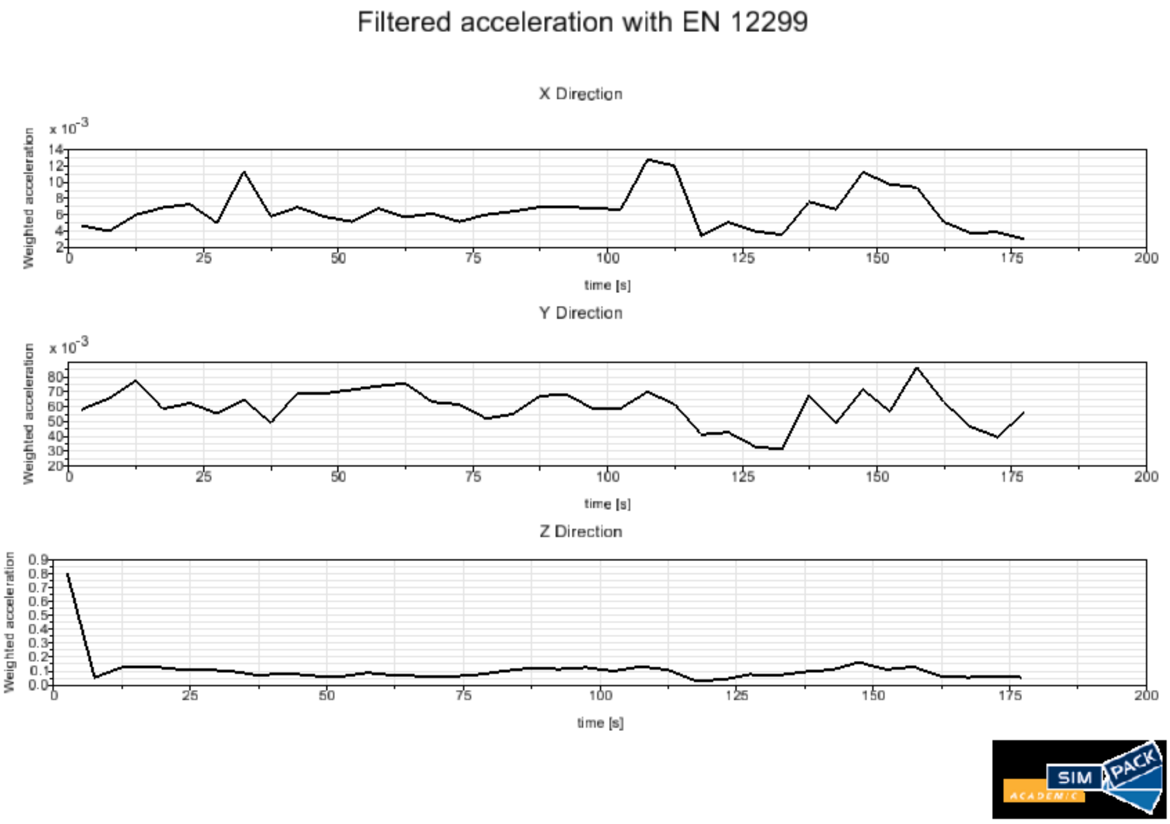

Figure 51 - Weighted accelerations, according to EN 12299 [52], in x, y and z direction, by the simulation time [s].

From this data, N_{MV} can be calculated, resulting in the values in Table 21. All these values are below 1, which correspond to a "very comfortable level", as in Table 4.

Table 21 - N_{MV} results for the ride comfort analysis

N_{MVx}	N_{MVy}	N_{MVz}	N_{MV}
0.07	0.45	0.81	0.93

5.6 Behaviour in track with poor conditions

In this section, the rail car behaviour in a track with substandard condition will be evaluated. Similarly to what happened in the report done evaluating the accident which occurred in *Linha do Norte*, using the criteria in Table 22.

Table 22 - Criteria used to evaluate the behaviour of the rail car in track with bad condition, where Y is the lateral wheel force, Q is the vertical wheel force and Q_0 is the normal preload

Criteria	Definition	Limit	Filter
Nadal	$\xi_N = \frac{Y}{Q}$	0.8	Low-pass filter 20 Hz a and sliding mean method with - window length 2.0 m - step length ≤ 0.5 m
Proud'Homme	$\xi_P = \frac{\sum_e \mathrm{Y}}{10 + \frac{2Q_0}{3}}$	1.0	
Unloading	$\xi_D = 1 - \frac{Q}{Q_0}$	0.9	none

Since the most critical section of track is a left turn, for the Nadal criteria will be considered the right wheel of the front wheelset for the analysis, whereas for the unloading criteria will be considered the left wheel of the same wheelset. Although the accident occurred at 90 km/h, this simulation was done for several speeds: 90 km/h; 100 km/h; 120 km/h; 140 km/h; 160 km/h; 180 km/h; and 200 km/h. The results of these analysis are shown in Figure 52, Figure 53 and Figure 54.

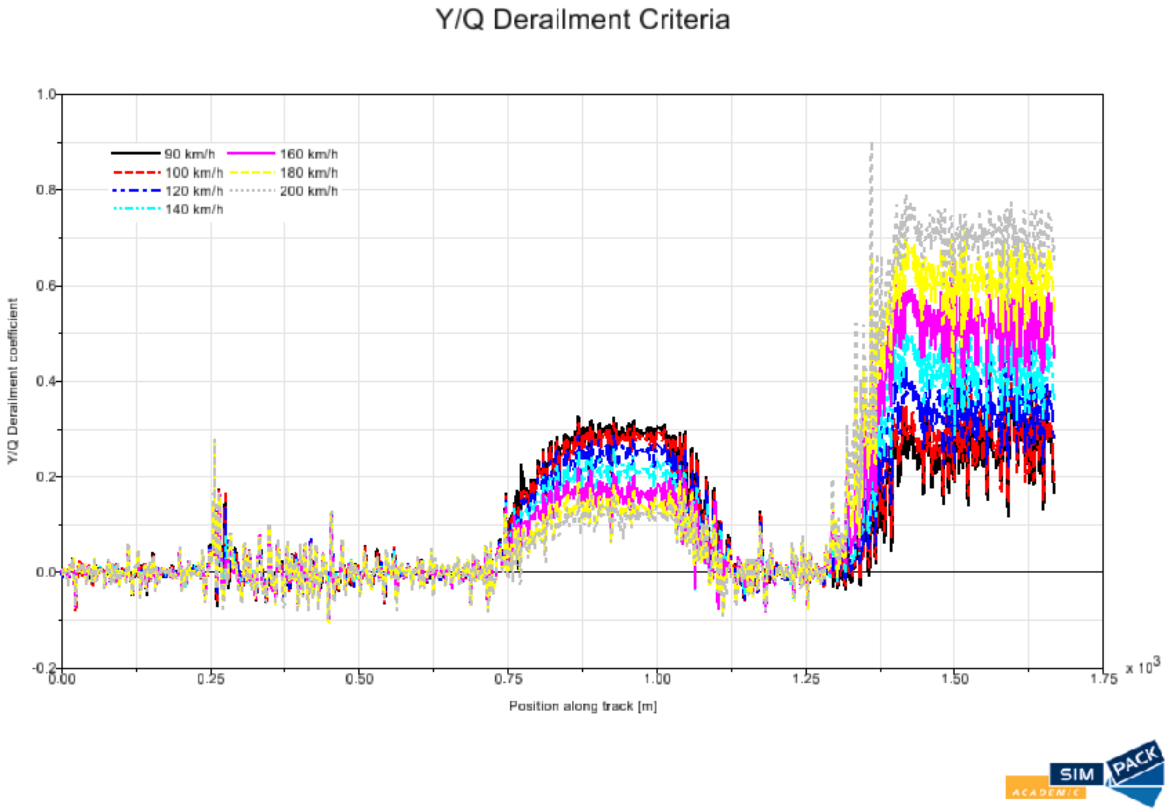

Figure 52 - Nadal criteria results, along the track, considering different speeds.

Regarding the Nadal criteria one can see that this criterion is fulfilled for every speed except in a point at 200 km/h. As expected, the criteria value increases with the increase of the speed in the final section of track (left turn).

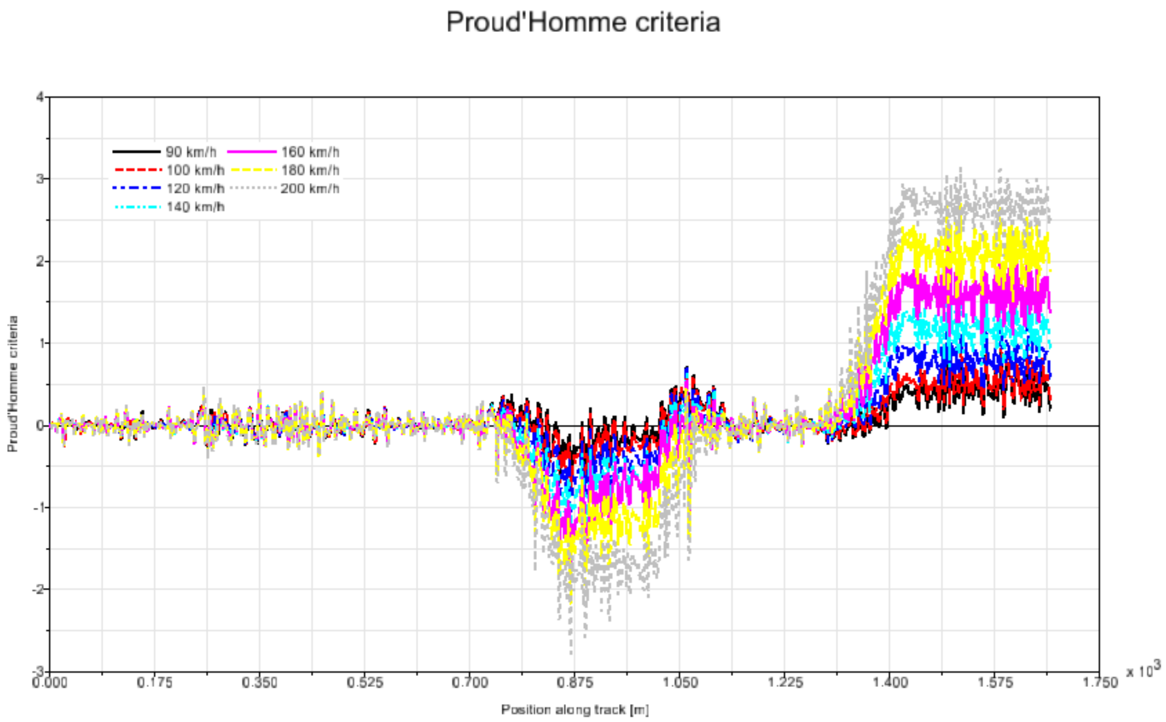

Figure 53 - Proud'Homme criteria results, along the track, considering different speeds.

In the case of the Proud'Home criteria, which results can be seen in Figure 53, these are much less satisfactory. According to this criterion at speeds over 120 km/h, there will be risk of derailment. Even at 120 km/h there are result points with value higher than 1.

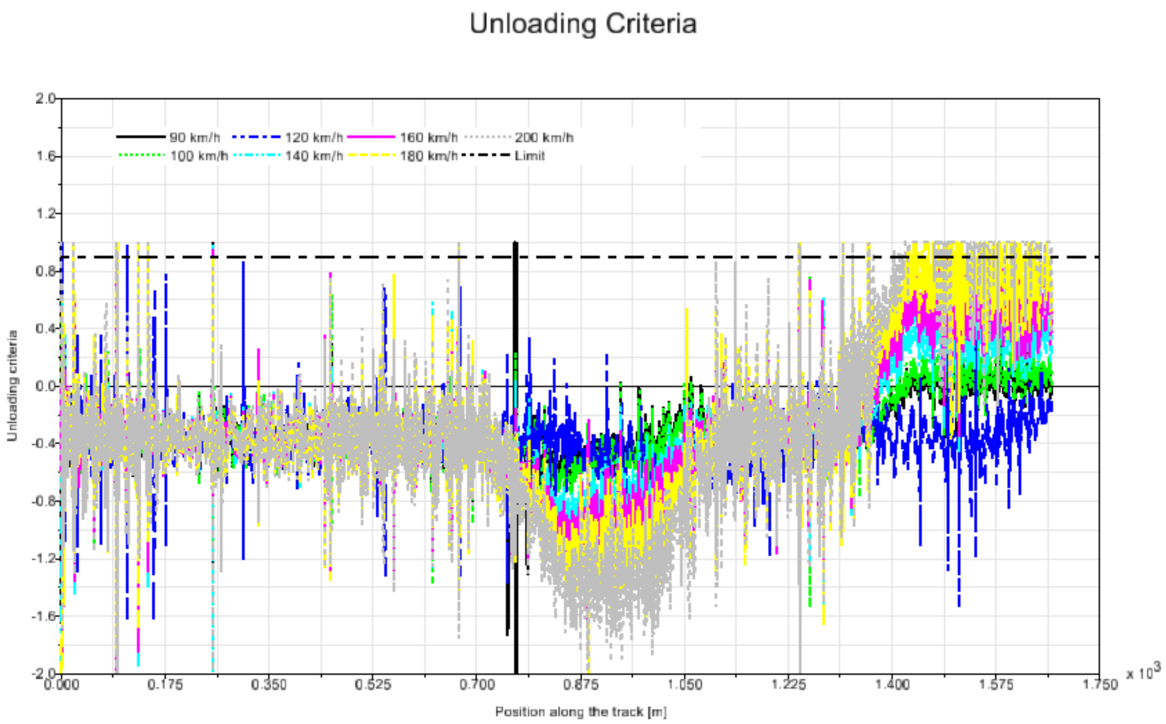

Figure 54 - Unloading criteria results, along the track, considering different speeds.

The final analysis, the unloading criteria, with results in Figure 54, have the worst performance. In this criterion at every speed there are points that exceed the limit value. This is more critical for speeds above 160 km/h.

From these 3 criteria can be deduce that the behaviour of this rail car in a similar situation to the one occurred would not lead to the same result. It is relevant that a freight wagon has a different behaviour from a passenger wagon. The fact that passenger wagon has a secondary suspension will lead to a much less stiffer suspension which may help the behaviour in curve. The existence of a secondary suspension will also allow the dimensioning of each suspension steps (primary and secondary) to absorb different frequencies. By nature, passenger railcars have better capabilities when dealing with rail deficiencies.

6 Conclusion

The rail passenger design has evolved with the railway industry. The evolution of the infrastructure allowed the growth of rail cars capacity. The development of rail vehicle dynamics led to the increase of the maximum speed of train currently. The increase in requirements and the standardization in design led to a defined and extensive set of tests for the certification of new models and manufacturers.

Multi-body dynamics is a complex area of studies with constant developments. It was concluded that there are several models defined in the literature that could be implemented in each application. For each element, the dynamic behaviour should be analysed, so it can be properly modulated in the multi-body model. It was also concluded that spring and damper simulation are usually done by non-linear stiffness and damping functions.

After researching the background of ARCO passenger cars, it was determined that the dynamic specifications were changed 10 years after the original manufacture, allowing for better performances. The use of computational tools allowed for the estimation of the mass properties of each body. The models described in the theoretical background allowed for the determination of both the stiffness and damping of the suspension elements. Consulting manufacturers data is essential for the modelling of the rail car, specially the suspension elements.

In order to obtained results for several characteristics of the model, it is necessary to design different experiments. Different track layouts and simulation settings will allow the dynamic performance testing, namely: i) the critical speed determination; ii) the ride comfort lever; iii) and the behaviour in a track in poor condition. Different test speeds can also be necessary.

From the results of simulations, one can conclude that the added anti-yaw dampers allowed a great increase in the critical speed of the rail car, reaching 390 km/h. Also, it can be concluded that without the anti-yaw dampers, the critical speed is too low, 120 km/h, when it should be higher than 160 km/h, considering the manufacturers specification, which can be explained by the accuracy of the suspension elements modelling or the considered mass distribution.

Regarding, the dynamic behaviour of the rail car, this pointed out that the maximum admissible speed of the proposed model is 160 km/h. Such a difference from the predicted admissible speed of 200 km/h, corresponding to the admissible speed of the ARCO passenger rail car. In addition, this can mean that although in straight tracks and large radius curves the results are acceptable, in small radius curves the maximum speed is lower. The lateral forces are above the expected, which could mean an overload of the rails.

In terms of ride comfort, it can be inferred that the ARCO passenger car offers a notably high level of comfort based on the criteria outlined in the relevant standard. It attains a classification of "Very Comfortable," even when traversing less than ideal track conditions.

Ultimately, the performance observed in a real track section model surpassed that of the locomotive involved in the accident, demonstrating a greater ability to maintain higher speeds without derailing. However, it is worth noting that the model exhibits certain dynamic characteristics that fall short of those attributed to the actual passenger car. This discrepancy could be attributed to either oversimplifications in the modelling process or the reliance on certain assumptions when official data was unavailable.

6.1 Future works

Using this model as a starting point, should be done a more extensive parametric analysis with the aim of understanding the influence each parameter has in the dynamic behaviour of the passenger car.

The next step of this analysis, once there are the necessary resources, would be instrumentation of an ARCO passenger car, in order to perform a comparison between the numerical and experimental results. In the future, should be done a more precise description of the suspension elements, for a more accurate model of the ARCO passenger car. Determining the model properties which contain more uncertainty defining an objective function, preform an optimization to approximate the model response to the real one.

Besides the already done analysis, a track representative of the cycle of the rail car could be developed to solve a concrete problem of the company regarding fatigue defects appearing near the mount of the anti-yaw dampers, which were added several years after the original manufacture.

Finally, the model could also be study alternative software of multi-body dynamics, as well as, the influence different simulation parameters would have on the result.

References

1. European Comission, *The European Green Deal*. 2019.
2. Assembleia da República, *Lei n.º 98/2021, de 31 de dezembro, Lei de Bases do Clima*. 2021: Diário da República n.º 253/2021, Série I de 2021-12-31, páginas 5 - 32.
3. Governo de Portugal, *ROTEIRO PARA A NEUTRALIDADE CARBÓNICA 2050 (RNC2050)*, Ministério do Ambiente e Transição Energética, Editor. 2019.
4. European Comission, *Proposal for a REGULATION OF THE EUROPEAN PARLIAMENT AND OF THE COUNCIL on Union guidelines for the development of the trans-European transport network, amending Regulation (EU) 2021/1153 and Regulation (EU) No 913/2010 and repealing Regulation (EU) 1315/2013*. 2022.
5. Ministério das Infraestruturas e Habitação, *Plano Ferroviário Nacional-Diagnóstico da Situação Territorial*. 2022.
6. Cipriano, C., et al., *A que velocidade anda o Ferrovia 2020?*, in *Público*. 2023, PÚBLICO Comunicação Social SA.
7. Ministério do Planeamento e Infraestruturas, *Plano de investimentos em infraestruturas Ferrovia 2020*. 2016.
8. Governo de Portugal, *Programa Nacional de Investimentos 2030*. 2020.
9. AMA – Agência para a Modernização Administrativa, I.P. *Projeto PRR - PRODUZIR MATERIAL CIRCULANTE FERROVIÁRIO EM PORTUGAL* Mais Transparência 2023 01/06/2023]; Available from: https://transparencia.gov.pt/pt/fundos-europeus/prr/beneficiarios-projetos/projeto/02-C05-i01.02-2022.PC645644454-00000065/#project_prr_form_id.
10. Cipriano, C., *CP fecha 2022 com os primeiros lucros da sua história*, in *Publico*. 2023, PÚBLICO Comunicação Social SA.
11. CP - Comboios de Portugal E.P.E. *A Empresa*. 2023 01/06/2023]; Available from: https://www.cp.pt/institucional/pt/empresa.
12. Cipriano, C., *CP já pode avançar com concurso público para a compra de novos comboios* in *Público*. 2020.
13. Cipriano, C., *Maior compra de comboios da história da CP tem seis candidatos* in *Público*. 2022.
14. Nunes, D.F., *Governo atira compra de comboios de alta velocidade para lançamento de obras no Porto-Lisboa* in *Eco*. 2023.
15. Cipriano, C., *CP está a ficar sem comboios e à beira do colapso*, in *Público*. 2018, Público.
16. Nunes, D.F., *CP recupera cerca de 170 unidades em 2022*, in *Dinheiro Vivo*. 2021: Portugal.
17. Stacey, J., *A brief history of the railways*. 2018, Rail Discoveries.
18. Lewis, M. *Railways in the Greek and Roman world*. in *Early railways: a selection of papers from the First International Early Railways Conference*. 2001.
19. Bailey, M., *The history of tracks and trains: a lesson in joined-up thinking*. Proceedings of the Institution of Civil Engineers - Civil Engineering, 2005. **158**(3): p. 134-142.
20. Thomas Clark Shedd, J.E.V., Geoffrey Freeman Allen, *railroad*, in *Encyclopedia Britannica*. 2023.

21. *Steam train anniversary begins*, in *BBC News*. 2004.

22. Association pour la connaissance des Travaux Publics. *From 1800 to 1850 in England*. History of railways 2008; Available from: https://www.planete-tp.com/en/from-1800-to-1850-in-england-a531.html.

23. Grubler, A., *The rise and fall of infrastructures: dynamics of evolution and technological change in transport*. 1990: Physica-Verlag.

24. Association pour la connaissance des Travaux Publics. *1850 to 1870*. History of railways 2008; Available from: https://www.planete-tp.com/en/1850-to-1870-a533.html.

25. Duffy, M.C., *Electric Railways: 1880-1990*. 2003: Iet.

26. *MOTIVE POWER FOR BRITISH RAILWAYS.* The Engineer, 1956. **202**(5248).

27. Armand, L., *Motive Power Trends on European Railways.* Proceedings of the Institution of Mechanical Engineers, 1947. **157**(1): p. 239-245.

28. Union Passific. *Diesel-Electric Locomotives*. 2016; Available from: https://www.up.com/aboutup/special_trains/diesel-electric/.

29. Iwnicki, S., *Handbook of railway vehicle dynamics*. 2006: CRC press.

30. Knothe, K. and S. Stichel, *Rail vehicle dynamics*. 2017: Springer.

31. Klingel, W., *Uber den Lauf der Eisenbahnwagen auf gerader Bahn.* Organ fur die Fortschritte des Eisenbahnwesens in technischer Beziehung, 1883.

32. Wickens, A.H., *The dynamics of railway vehicles—from Stephenson to Carter.* Proceedings of the Institution of Mechanical Engineers, Part F: Journal of Rail and Rapid Transit, 1998. **212**(3): p. 209-217.

33. Redtenbacher, F., *Die gesetze des lokomotiv-baues*. 1855: Bassermann.

34. Knothe, K., *History of wheel/rail contact mechanics: from Redtenbacher to Kalker.* Vehicle System Dynamics, 2008. **46**(1-2): p. 9-26.

35. Knothe, K. and F. Böhm, *History of Stability of Railway and Road Vehicles.* Vehicle System Dynamics, 1999. **31**(5-6): p. 283-323.

36. Boedecker, C., *Die Wirkungen zwischen Rad und Schiene und ihre inflüsse auf den Lauf und den ewegungswiderstand der Fahrzeuge in den Eisenbahnzügen (The effects between wheel and rail and their influences on the running behavior and the resistance of vehicles in railway trains)*. 1887: Hahn.

37. European Union Agency for Railways, *Interoperability Overview 2023*. 2023.

38. European Committee for, S., *Railway applications gauges EN 15273-1: 2013 Part 1 general-common rules for infrastructure and rolling stock.* 2013, Brussels: CEN. 218 p.-218 p.

39. European Union Agency for Railways, <*Guide for the application of the INF TSI (EN)_1.pdf*>. Guide for the application of the INF TSI.

40. OpenStreetMap. *OpenRailwayMap*. 01/09/2023]; Available from: https://openrailwaymap.org/index.php.

41. Guigon, M., et al., *High-Speed Rail Atlas*. 2022, Geography and Railway Traffic Research Group, Fundación de los Ferrocarriles Españoles (FFE).

42. UIC and Union Internationale des Chemins de fer, *HIGH-SPEED AROUND THE WORLD*, in *Historical, geographical and technological development*. 2023, UIC Passenger Department.

43. UIC, U.I.d.C.d.f. *High-Speed Rail History*. 2015 Available from: https://uic.org/passenger/highspeed/article/high-speed-rail-history.

44. UIC and Union Internationale des Chemins de fer, *Design a better future vision of rail-2030*. 2021.

45. Paiva, F.d.B., *Evolução dos caminhos de ferro*.

46. Portugal, C.P.-C.d. *Cronologia da história dos caminhos de ferro em Portugal*. 2021 31/05/2023]; Available from: https://www.cp.pt/institucional/pt/cultura-ferroviaria/historia-cp/cronologia.

47. Leite, J., *Sorefame*. 2014: Resto de coleção.

48. Lusa, *Aprovada integração da EMEF na Comboios de Portugal* in *Publico*. 2023, PÚBLICO Comunicação Social SA.

49. Spiryagin, M., et al., *Design and simulation of rail vehicles*. 2014: CRC press.

50. Okamoto, I., *How bogies work.* Japan railway & transport review, 1998. **18**: p. 52-61.

51. European Committee for Standardization, *EN 14363: 2016 - Railway applications testing and simulation for the acceptance of running characteristics of railway vehicles running behaviour and stationary tests* 2016, CEN: Brussels.

52. European Committee for Standardization, *EN 12299: 2023 - Railway applications - Ride comfort for passengers - Measurement and evaluation* 2023, CEN: Brussels.

53. ISO - International Organization for Standardization, *ISO 2631-1:1997 - Mechanical vibration and shock — Evaluation of human exposure to whole-body vibration*. 2023, CEN: Brussels.

54. Portugal Instituto Português da, Q., *Vibrações mecânicas e choque avaliação da exposição do corpo inteiro e vibrações Parte 1 requisitos gerais NP ISO 2631-1: 2007*. 37 p-37 p.

55. Rodrigues, J.D., *Apontamentos de Vibrações de Sistemas Mecânicos*. 2021, Faculdade de Engenharia da U.PORTO, Departamento de Engenharia Mecânica.

56. Bruni, S., et al., *Modelling of suspension components in a rail vehicle dynamics context.* Vehicle System Dynamics, 2011. **49**(7): p. 1021-1072.

57. European Committee for, S., *Cylindrical helical springs made from round wire and bar calculation and design EN 13906-1: 2013 Part 1 compression springs*. 2013, Brussels: CEN. 35 p-35 p.

58. Krettek, O. and M. Sobczak, *Zur Berechnung der Quer-und Biegekennung von Schraubenfedern für Schienenfahrzeuge.* ZEV-Glas. Ann, 1988: p. 319-326.

59. Wang, W.L., et al., *Rail vehicle dynamic response to a nonlinear physical 'in-service' model of its secondary suspension hydraulic dampers.* Mechanical Systems and Signal Processing, 2017. **95**: p. 138-157.

60. CP - Comboios de Portugal E.P.E. *ARCO*. 2022 15/05/2023]; Available from: https://www.cp.pt/institucional/pt/cultura-ferroviaria/frota-material-circulante/arco.

61. Cipriano, C., *CP triplica número de carruagens a comprar a Espanha* in *Público*. 2020.

62. Cipriano, C., *Carruagens rejeitadas por Espanha já estão prontas para resolver problemas na CP*, in *Público*. 2021, Público.

63. Nunes, D.F., *CP pode pôr a circular carruagens compradas a Espanha* in *Eco*. 2021: Portugal.

64. Marco, A., *Los coches 10000*, in *Viajando en tren* 1999.

65. *Serie 10.000, los coches clásicos de departamentos de Renfe*, in *Via Libre - La revista del ferrocarril*. 1999, Fundación de los Ferrocrriles Españoles

66. RENFE Mantenimiento de Material Rodante, *Norma Tecnica De Mantenimiento*. 1994.

67. Eickhoff, B.M., J.R. Evans, and A.J. Minnis, *A Review of Modelling Methods for Railway Vehicle Suspension Components.* Vehicle System Dynamics, 1995. **24**(6-7): p. 469-496.

68. KONI, *Global solutions for the railway industry*. 2014.

69. Duym, S., R. Stiens, and K. Reybrouck, *Evaluation of Shock Absorber Models.* Vehicle System Dynamics, 2007. **27**(2): p. 109-127.

70. Kasteel, R.V., et al., *A new shock absorber model for use in vehicle dynamics studies.* Vehicle System Dynamics, 2005. **43**(9): p. 613-631.

71. Mousavi Bideleh, S.M. and V. Berbyuk, *Global sensitivity analysis of bogie dynamics with respect to suspension components.* Multibody System Dynamics, 2016. **37**(2): p. 145-174.

72. Alonso, A., J.G. Giménez, and E. Gomez, *Yaw damper modelling and its influence on railway dynamic stability.* Vehicle System Dynamics, 2011. **49**(9): p. 1367-1387.

73. Ribeiro, D.R.F., *Efeitos dinâmicos induzidos por tráfego em pontes ferroviárias: modelação numérica, calibração e validação experimental.* 2012.

74. Manashkin, L., S. Myamlin, and V. Prikhodko, *Oscillation dampers and shock absorbers in railway vehicles (Mathematical models)*. 2010: Ministry of Transport and Communication of Ukraine.

75. Zhang, T. and H. Dai, *On the nonlinear dynamics of a high-speed railway vehicle with nonsmooth elements.* Applied Mathematical Modelling, 2019. **76**: p. 526-544.

76. Oliveira, H.R., *Modelação e Análise Estrutural dos Bogies das Carruagens ARCO*. 2023.

77. Edu, D.E., *Simpack Rail*. 2023.

78. Faculdade de Engenharia da Universidade do Porto - Centro de Saber da Ferrovia, *Avaliação e Simulação Numérica do Descarrilamento do Comboio de Mercadorias na Linha do Norte a 01-04-2017*. 2020.

79. Gabinete de Prevenção e Investigação de Acidentes com Aeronaves e de Acidentes Ferroviários, *Descarrilamento de comboio de mercadorias na Linha do Norte, próximo de Adémia, em 01-04-2017*. 2019.